Received: 2 May 2021 | Accepted: 19 June 2021

DOI: 10.1111/gcb.15764

Global Change Biology WILEY

PRIMARY RESEARCH ARTICLE

Tree hazards compounded by successive climate extremes after masting in a small endemic tree, *Distylium lepidotum*, on subtropical islands in Japan

Tomomi Nakamura[1] | Atsushi Ishida[1] | Kiyosada Kawai[1,2] | Kanji Minagi[1] | Shin-Taro Saiki[3] | Kenichi Yazaki[4] | Jin Yoshimura[5,6,7]

[1]Center for Ecological Research, Kyoto University, Otsu, Shiga, Japan

[2]Japan International Research Center for Agricultural Sciences, Tsukuba, Ibaraki, Japan

[3]Forestry and Forest Products Research Institute, Tsukuba, Ibaraki, Japan

[4]Hokkaido Research Center, Forestry and Forest Products Research Institute, Sapporo, Hokkaido, Japan

[5]Institute of Tropical Medicine, Nagasaki University, Nagasaki, Nagasaki, Japan

[6]Faculty of Science, Tokyo Metropolitan University, Hachioji, Tokyo, Japan

[7]The University Museum, The University of Tokyo, Bunkyo, Tokyo, Japan

Correspondence
Atsushi Ishida, Center for Ecological Research, Kyoto University, Otsu, Shiga 520-2113, Japan.
Email: atto@ecology.kyoto-u.ac.jp

Funding information
Japan Society for the Promotion of Science, Grant/Award Number: 16H02708 and 18H04149

Abstract

Ongoing global warming increases the frequency and severity of tropical typhoons and prolonged drought, leading to forest degradation. Simultaneous and/or successive masting events and climatic extremes may thus occur frequently in the near future. If these climatic extremes occur immediately after mass seed reproduction, their effects on individual trees are expected to be very severe because mass reproduction decreases carbohydrate reserves. While the effects of either a single climate extreme or masting alone on tree resilience/growth have received past research attention, understanding the cumulative effects of such multiple events remains challenging and is crucial for predicting future forest changes. Here, we report tree hazards compound by two successive climate extremes, a tropical typhoon and prolonged drought, after mass reproduction in an endemic tree species (*Distylium lepidotum* Nakai) on oceanic islands. Across individual trees, the starch stored within the sapwood of branchlets significantly decreased with reproductive efforts (fruit mass/shoot mass ratio). Typhoon damage significantly decreased not only the total leaf area of apical shoots but also the maximum photosynthetic rates. During the 5-month period after the typhoon, the mortality of large branchlets (8–10-mm diameter) increased with decreasing stored starch when the typhoon hit. During the prolonged summer drought in the next year, the recovery of total leaf area, stored starch, and hydraulic conductivity was negatively correlated with the stored starch at the typhoon. These data indicate that the level of stored starch within branchlets is the driving factor determining tree regrowth or dieback, and the restoration of carbohydrates after mass reproduction is synergistically delayed by such climate extremes. Stored carbohydrates are the major cumulative factor affecting individual tree resilience, resulting in their historical effects. Because of highly variable carbohydrate levels among individual trees, the resultant impacts of such successive events on forest dieback will be fundamentally different among trees.

Atsushi Ishida and Tomomi Nakamura are equally contributed.

KEYWORDS
carbon starvation, drought, hydraulic failure, masting, oceanic islands, tropical storm, water relations

1 | INTRODUCTION

In recent decades, climate-driven forest degradation has been widespread over multiple biomes (e.g., Abrams & Nowacki, 2016; Allen et al., 2010; Anderegg et al., 2020; Bennett et al., 2015), resulting in severe damage to forest ecosystems globally. Climate extremes have intensive effects on gross primary production, structure, and function in terrestrial forest ecosystems (Hoffmann et al., 2011; Reichstein et al., 2013; Williams et al., 2013; Xu et al., 2019). Climate models project increases in the frequency and intensity of droughts and tropical typhoons/cyclones (Oouchi et al., 2006). Global warming thus brings new hazards through the novel combination of prolonged droughts and more frequent and intense typhoons.

Many tree species undergo masting phenology for regeneration, and relatively long nonflowering periods may occur in individual trees (e.g., Ascoli et al., 2017; Bogdziewicz et al., 2020, 2021; Fernández-Martínez & Peñuelas, 2011; Kelly & Sork, 2002; LaMontagne et al., 2020; Pearse et al., 2017; Vacchiano et al., 2017). In masting years, blooming trees pay huge resource costs for massive seed production, requiring nonnegligible investments in stored carbohydrates and nitrogen (Han et al., 2011, 2014; McDowell et al., 2000; Miyazaki, 2013; Newell, 1991). In addition, some masting trees also frequently reduce subsequent annual ring growth and reproduction as delayed costs (Bell, 1980; Kabeya et al., 2017; Miyazaki, 2013; Obeso, 2002). In contrast, negative trade-offs between vegetative or radial growth and reproduction are not detected in some tree species (Fernández-Martínez et al., 2012; Koenig et al., 2020; Vergotti et al., 2019) or such phenomena are due to apparent trade-offs (not causal; Knops et al., 2007). In addition, the effects of climate change on masting frequency are predicted to be diverse (Pearse et al., 2017), including increases (Shibata et al., 2020) and no change or decreases (Kelly et al., 2013) in the fecundity frequency. The controversy also involves biotic effects, such as the capacity of acclimating to climate change (Bogdziewicz, Fernández-Martínez, et al., 2020) and forest stand ageing (Pesendorfer et al., 2020).

Therefore, we currently have a poor understanding of how and where frequency of masting will decrease or increase, whereas climatic extremes are expected to increase in frequency with the progression of ongoing climate change (Ascoli et al., 2017). However, if massive seed reproduction largely decreases the carbohydrate reserves, climate extremes that occur after masting are likely to lead to intensive tree declines. Such successive events may increase forest degradation and inhibit regeneration and reforestation. The impact of a single extreme climate event or a single masting event on adult tree growth/resilience has been widely studied. In contrast, the compound effects of climate extremes after masting in forest ecosystems and their underlying physiological mechanisms remain unclear, hindering the prediction of the impacts of multiple events caused by long-term climate change.

Understanding the physiological mechanisms of tree decline caused by climate extremes is crucial for predicting forest degradation and improving global models. To date, two major nonpathogen-related hypotheses concerning drought-induced tree death have been proposed: (1) hydraulic failure; and (2) carbon starvation. The hydraulic failure hypothesis postulates that tree die-offs are largely a result of dysfunctional water transport caused by xylem embolism, creating high tension in xylem conduits when water loss from leaves is higher than soil water uptake (Anderegg et al., 2012; Davis et al., 2002; McDowell et al., 2008; Nardini et al., 2013; Rowland et al., 2015; Sperry et al., 1988). The carbon starvation hypothesis suggests that tree die-offs are caused by shortages of carbohydrate reserves resulting from a decline in photosynthesis when stomata are entirely closed under drought (Kono et al., 2020; McDowell et al., 2008; O'Brien et al., 2014; Saiki et al., 2017). Although the two hypotheses have been debated, recent advances offer a coupling of both hypotheses due to reciprocal physiological processes (Hartmann, 2011; Hillabrand et al., 2019; Sala et al., 2010; Sevanto et al., 2014; Yoshimura et al., 2016; Zeppel et al., 2013), proposing an integrated schematic model for the physiological process of drought-induced tree death (Kono et al., 2020). Here, we ask the following questions: (1) How do different types of disasters after masting cause physiological tree damage? (2) How does lingering damage caused by successive climate extremes after masting lead to tree decline?

Recently, subtropical evergreen forests in the Ogasawara (Bonin) Islands immediately experienced two types of disasters, typhoons and prolonged drought, after mass flowering over a period of 2 years (Figure 1a). The Ogasawara Islands, a World Natural Heritage site in Japan, are small oceanic islands located in the subtropical North Pacific Ocean approximately 1000 km south of Tokyo (Figure S1). On the islands, a small endemic evergreen tree species, *Distylium lepidotum* Nakai (Hamamelidaceae), had the mass flowering in winter from 2018 to 2019, and the fruits ripened in autumn to winter of 2019 (Figure 1c,d). During this masting, we found a large variation in the degree of seed production among individual trees. When their fruits were maturing, typhoon "Bualoi" hit the evergreen forests of the islands on October 24, 2019 (Figure 1b; Figure S1). An instantaneous maximum wind speed of 52.7 m s^{-1} was recorded on the islands, adding major damage to the forests due to the intense wind and salt spray from sea water. Subsequently, a prolonged drought struck the forests in the early summer in 2020 (Figure S2).

Here, we report the compound deadly tree hazards caused by two successive climate extremes, a tropical typhoon and prolonged drought, after mass flowering on oceanic islands. In individual

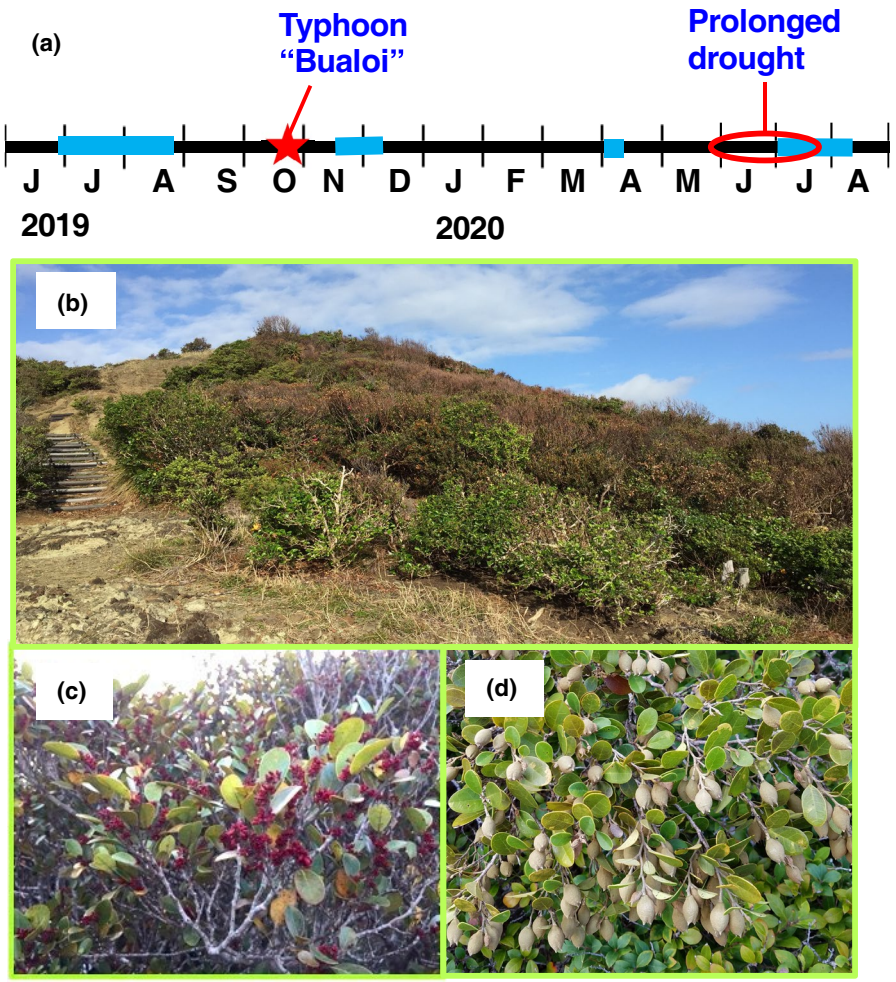

FIGURE 1 Time schedule of field surveys in relation to masting, the typhoon, and prolonged drought. (a) Time schedule. Mass flowering started in the winter of 2018–2019, and the fruits ripened from autumn to winter in 2019. Typhoon "Bualoi" hit the evergreen forests of the Ogasawara (Bonin) Islands on October 24 2019. Under prolonged drought, the dry days (<7 mm in daily precipitation) continued from May 30 to July 19 in summer 2020. The light blue bars show the days of field observation. (b) Overview of the study site approximately 1 month after the typhoon hit (photograph on November 28, 2019), indicating damaged branches and leaves (brown-colored areas). The right direction is the windward sea side. (c, d) Mass flowering and fruiting, respectively, in *Distylium lepidotum* Nakai trees

trees of *D. lepidotum*, we have periodically examined the parameters related to hydraulic failure and carbon starvation over 2 years. Therefore, tree regrowth or dieback was determined by the restoration of carbohydrate levels which was synergistically delayed by climate extremes after masting. Stored carbohydrates are thus the major factor of cumulative historical effects on individual tree resilience.

2 | METHODS

2.1 | Method overview

Distylium lepidotum Nakai (Hamamelidaceae) is a small endemic tree species with typical masting phenology in the Ogasawara (Bonin) Islands. Our long-term forest survey (1987–2020) of the Ogasawara (Bonin) Islands (a World Natural Heritage site) indicated that this species has a clear masting phenology (personal communication). During fruiting in the early summer of 2019 (before the typhoon hit), we first selected nine individual trees of *D. lepidotum* with different levels of seed production. The top canopy heights above the ground were less than 2.6 m (Table S1). In each selected tree, the seed production levels (i.e., reproductive effort) and the degrees of typhoon damage were evaluated. Since then, we have periodically examined the nonstructural carbohydrates (NSCs) within sapwood and the hydraulic conductivity in branchlets, the dark respiration rates by standardized at 26°C, and the total leaf areas (as new leaf production) in the apical canopy shoots. To examine the effects of typhoon damage after masting on tree dieback, the mortality rates of branchlets of the apical shoots among different diameter classes were also examined in early April 2020 (approximately 5 months after the typhoon).

2.2 | Study site, plant materials, and seed production

The Ogasawara Islands are oceanic islands in the northern Pacific Ocean. The study site (27°06′N, 142°13′E, elevation 130–160 m above sea level) was set on Chichi-jima Island, one of the territorial islands of Ogasawara. This study site is located on a southeast-facing slope (Figure 1b). The bedrocks are exposed in several places. From 2011 to 2020, the mean air temperature of the islands was 23.5°C, and the mean annual precipitation was 1014 mm (observations by the Japan Meteorological Agency). The soil in the study site is of volcanic origin. The soil pH ranges from 4.6 to 5.3 (Morita, 1981).

There are no records of snow falling on the islands. Forest fires do not occur on the islands.

A field survey was conducted four times: in summer (July and August) and winter (November and December) in 2019 and in spring (April) and summer (July and August) in 2020 (Figure 1a). *D. lepidotum* trees exhibited mass flowering in winter from 2018 to 2019, and the fruits ripened in autumn to winter of 2019 (Figure 1c,d). Nine individual trees with different amounts of seed production were selected in summer in 2019 before typhoon "Bualoi" hit (Table S1).

To examine the seed production levels among the individual trees, three to six apical shoots were collected from each tree (Figure S3a). The collected shoots were dried (60℃, >72 h). The ratio of fruit mass to the total shoot mass was measured as the reproductive effort for each shoot (Figure S3c,e). The mean values for the apical shoots were used as the reproductive effort for each individual tree.

2.3 | Subsequent typhoon damage

On October 24, 2019, Typhoon "Bualoi" hit the Ogasawara Islands (Figure S1). During the event, the minimum air pressure was 963.5 hPa and the instantaneous maximum wind speed was 52.7 m s^{-1} on Chichi-jima Island. The top canopies received intensive damage caused by strong winds and intense salt spray from sea water, especially on the windward sea sides (Figure 1b; Figure S3b). However, the degrees of typhoon damage varied visually among the individual trees according to the differences in micro-locations and top canopy heights.

To evaluate the effects of typhoon and salt spray damage on the individual trees, we compared the values of electrolyte leakage in the top canopy leaves before and after the typhoon (Figure S3d). We collected the top canopy leaves from three apical shoots per tree, and the electrolyte leakage in each leaf was measured to evaluate cell membrane damage (Blum & Ebercon, 1981). Whole leaves were put into a 10-ml vial bottle one by one, and the bottles were filled with deionized water until the leaf samples were completely soaked. Approximately 24 h later at room temperature, the electrical conductivity in the solution was measured with a compact electrical conductivity meter (LAQUAtwin-EC-33B; HORIBA Co. Ltd.). Subsequently, the bottles were placed into a chamber (HR-P07; KOM Corporation) and then heated for 40 min at 70 kPa to breck all leaf cells. After heating, the bottles were cooled for approximately 2 h in the laboratory room, and then the electrolyte conductivity in the solution was measured again. The values of electrolyte conductivity for completely damaged leaves were not known. Thus, using completely broken leaves, we further corrected the values of leaf electrolyte leakage as follows.

Ten leaves were randomly collected from the field, and the leaves were placed in a freezer (−20°C, >48 h) to break all leaf cells. Then, the ratios of electrolyte conductivity before and after heating (ECRs) were obtained using freshly frozen leaves. Even in completely broken leaves, the ratio was 0.755 ± 0.048 (mean ± 1 SD), resulting in a correlation efficiency of 1.325 (=1/0.775). Therefore, the "corrected" electrolyte conductivity ratio (ECR) was given as follows:

$$ECR=1.325\times ECR \quad (1)$$

Based on correlation efficiency, the value of the electrolyte conductivity ratio of completely broken leaves is 1. The typhoon damage caused to individual trees was evaluated as the average values of the corrected electrolyte conductivity ratio for six leaves collected from three apical shoots. No significant correlation was found between reproductive effort and the typhoon damage among the examined trees, indicating that reproductive effort and typhoon damage were independent of each other (Figure S3f).

2.4 | Leaf water potential and soil depth

To evaluate soil drying in the summers of 2019 and 2020, the predawn (3:30–5:00) leaf water was periodically measured with a pressure chamber (1505D-EXP; PMS Instrument Company; Figure S2). The soil thickness around the nine surveyed trees was also evaluated with a manually operated dynamic cone penetrometer (S06-M; TUKUBA-MARUTO Co., Ltd.; Figure S4). The apparatus consisted of four parts: a top cone with a sharp (60°) angle and a diameter of 25 mm, a guide rod, a knocking head, and a 5-kg weight. The top cone was set on the ground surface beside the stem base of the individual trees, and the weight was continuously dropped at 0.5-m depths along the guide rod every time. Then, the depth (length) at which the top cone went down into the soil was measured for each drop of the weight until the top cone did not drop when it reached the base rock. The range of soil thickness was 0.07–1.02 m (Table S1). Because the length of the guide rod exceeded 1 m, we were fully able to measure the soil thickness.

2.5 | Leaf gas exchange

To examine the effects of reproductive effort and typhoon damage on leaf gas exchange, the maximum photosynthetic rates were measured in summer in 2019 (before the typhoon) and winter 2019 (after the typhoon) with a portable open gas exchange system (LI-6400; LI-COR Inc.). To avoid midday depression, all measurements were conducted before noon under near saturated light (2000 µmol m^{-2} s^{-1} photon flux density with red–blue light-emitting diodes) with 400 µmol mol^{-1} CO_2 in the inlet gas streams. The relative humidity in the outlet gas stream was adjusted to the relative humidity of the ambient air.

2.6 | Hydraulic conductivity and the percent loss of conductivity in branchlets

To examine the effects of reproductive effort, typhoon damage, and prolonged drought on branch hydraulics, the hydraulic conductivity was measured three times in summer in 2019 (before the typhoon), winter 2019 (after the typhoon), and summer in 2020 (under

prolonged drought), following the method of Sperry et al., (1988). Shoot samples were cut as long as possible before dawn (3:30–5:00) and were recut under water in the field to avoid the possibility of artificially induced embolism. The collected shoots were immediately transported to our laboratory with the cut ends submerged in water and were enclosed in black plastic bags for approximately 2 h to relax the xylem tension. We then recut the cut ends of the shoots in water to obtain branch segments as long as possible without branching (approximately 8–20-cm length). After removal of the bark and phloem at both cut ends, each branch segment was connected individually to the tubing system. A hydraulic pressure of 5 kPa was applied to the end of the segment by placing a water bag containing 20 mM KCl solution at a height 0.5 m above the sample. The other end was connected to a plastic bottle on an electronic balance (MS204S; Metra Toledo Co. Ltd.) by a Tygon tube, and then the water flow rates from the segment were automatically measured with an electronic balance. Based on the water flow rates, the sapwood area, and the branch length, we calculated the hydraulic conductivity of the branchlets (K_{branch}; kg s^{-1} m^{-1} MPa^{-1}) of each tree. All measurements were performed under a constant temperature of approximately 26°C in the laboratory.

Subsequently, the percent loss of conductivity (PLC) was examined in the same branch segments to evaluate the role of air-induced embolism in decreasing K_{branch}. The branch segments were flushed with 20 mM KCl solution under 0.15 MPa for 15 min to remove air-induced xylem embolism, and then the water-flow rates were measured again to obtain the maximum xylem hydraulic conductivity (K_{max}). The values of PLC were calculated as follows:

$$PLC = \left(1 - \frac{K_{branch}}{K_{max}}\right) \times 100. \quad (2)$$

After the hydraulic measurements, the photographic images of the sapwood cross-section on the upper side of the cut end were obtained using a digital microscope (Dino-Lite; AnMo Electronics Corporation), and then the cross-sectional area of xylem sapwood was measured with the image processing software ImageJ (Schneider et al., 2012).

2.7 | Dark respiration rates

To evaluate the effects of reproductive effort and typhoon damage on the respiratory consumption of stored carbohydrates, the dark respiration rates of the shoots were measured in summer 2019 (before the typhoon), winter 2019 (after the typhoon), and summer 2020 (under prolonged drought). The other branches on the same shoots as those used for the measurements of hydraulic conductivity were used to evaluate the respiration rates to reduce additional damage to the examined trees. The dark respiration rates were evaluated in each tissue (leaves, fruits, and branchlets) as follows. First, the respiration rates of the whole shoots including leaves, fruits, and branchlets, were measured. Next, the leaves were removed from the shoots with scissors, the respiration rates were measured again, the fruits were removed and the rates were measured again. The plant samples were put into a closed plastic box (5 or 14.5 L in volume) with a small fan. The size of the plastic box was selected according to the volume or length of the plant samples, and then the box was covered with black cloth. To measure the temperature, chromel-alumel thermocouples were placed into the box together with the plant parts. We assumed that the plant temperature was in equilibrium with the air temperature in the box. The increasing rates in air CO_2 concentration in the box were measured for 5–10 min, using a nondispersive infrared CO_2 gas analyzer (GMP343, Vaisala Inc.) connected to a data logger (GL240; Graphtec Co. Ltd.). The dark respiration rates were measured at a room temperature of approximately 26°C in our laboratory. From the increasing rates of CO_2 concentration and the box volume, the dark respiration rates were calculated.

After the measurements, the plant samples were dried (60°C, >72 h), and then the dry mass was weighed. Dry mass-based respiration rates of leaves, fruits and branchlets were separately determined by subtracting the respiration rates in each measurement. Furthermore, the obtained values were standardized at 26°C by using Q_{10} = 2 to eliminate the possible errors caused by the variations in room temperature.

2.8 | Non-structural carbohydrate storage within sapwood

To examine the effects of reproductive effort, the typhoon, and prolonged drought on the source–sink balance of carbohydrates, the NSCs (starch and soluble sugars) stored within the sapwood in branchlets (8–10-mm diameter) were examined three times in summer and winter in 2019 and in summer in 2020 (Table S2). The same branchlets used for the hydraulic conductivity and dark respiration measurements were also used for evaluating NSCs. The bark and phloem were swiftly removed with a blade before drying in our laboratory. The pieces of collected sapwood were dried (60°C, >72 h), and then ground to a fine powder with a vibrating mill (Hi-speed Vibrating Sample Mill TI-100; CMT Co., Ltd). The powdered samples were extracted in 80% ethanol (v/v), the supernatant was extracted via centrifugation and the soluble sugar contents were quantified with the phenol–sulfuric acid method (Dubois et al., 1951). To determine the amount of starch, the remaining pellets were depolymerized to glucose by the addition of KOH, acetic acid, and amyloglucosidase buffer, and the extracted glucose was quantified with the mutarotase–glucose oxidase method (Glucose C-II test; Wako).

2.9 | Mortality rates of branchlets

The effects of reproductive effort and typhoon damage on branchlet mortality were examined in 3-diameter classes of branchlets (1–2-, 3–4-, and 8–10-mm diameters). At approximately 1 month following the typhoon, 100 shoots with 1–2-mm diameters, 100 shoots with

3–4-mm diameters, and 30 shoots with 8–10-mm diameters were labeled in each tree. Approximately 5 months after the typhoon hitting (spring in 2020), we investigated whether the labeled branchlets were dead or alive. The mortality rates during the 5-month period following the typhoon were calculated for each diameter class. The branchlets broken by intense wind were eliminated from the mortality rate calculations.

2.10 | Statistics and GLMs

All statistical analyses were conducted with the software package "R" (Ver. 3.5.3; R Development Core Team, 2019). The effects of reproductive effort (Figure 2) and typhoon damage (Figure 3) and the effects of stored starch (Figures 4c and 5) were statistically examined by linear regressions. Regression lines in these figures were drawn, depending on the significance levels (solid lines: $p < 0.05$; dashed lines: $0.05 \leq p < 0.08$ in marginal). The *r*- and *P*-values in regression analysis are shown in Table S4. Statistical differences in the respiration rates among the tissues (Figure 2h) and in the branchlet mortality rates among the diameter classes (Figure 4b) were analyzed using the Steel-Dwass test (nonparametric multiple comparison).

To identify the significant effects of reproductive effort, typhoon damage, and starch reserves on the branchlet mortality rates in each size class (1–2-, 3–4-, and 8–10-mm diameter), generalized linear models (GLMs) were constructed assuming Gaussian error distributions with identity link function (Figure 4a). The averaged values among branchlets for each individual tree were used for the reproductive effort and typhoon damage ($n = 9$), and the mortality rates were obtained for each individual tree ($n = 9$; Table S5). We could test only the effects of reproductive effort, typhoon damage, and starch reserves on the branch mortality of three size classes by GLMs because of sample size limitations (nine trees). We could also not test the four interactive terms among reproductive effort, typhoon damage, and starch reserves. We also could not test all the measured traits, such as photosynthesis, respiration, branch hydraulics, total leaf area, soluble sugar, and NSCs. The branchlet mortality rates in each diameter class (1–2, 3–4, 8–10 mm) were the response variables, and reproductive effort, typhoon damage, and the starch concentrations within sapwood after the typhoon hit (winter in 2019) were the explanatory variables (Table S3a). In best subset regressions, the most plausible models with the lowest Akaike's information criterion values were selected to explain the mortality rates (Table S3b).

3 | RESULTS

The effects of reproductive effort (before the typhoon) were investigated across the examined trees (Figure 2). Maximum photosynthetic rates were not significantly correlated with the reproductive efforts (Figure 2f). However, the leaf color of shoots with a high reproductive effort often changed to yellowish, showing low photosynthetic rates (Figure S5). The total leaf area of shoots decreased significantly with increases in the reproductive effort of individual trees, resulting from a decrease in the area of individual leaves rather than in the number of leaves attached to the shoots (Figure 2a–c). On the other hand, the overall shoot (including leaves, twigs, and fruits) respiration rates increased marginally ($p = 0.058$) with reproductive effort (Figure 2g), because of significantly higher respiration rates of immature fruits than those of leaves and stems (Figure 2h). Although the soluble sugar concentrations within sapwood increased marginally with reproductive effort ($p = 0.063$; Figure 2d), the stored starch concentrations decreased significantly with reproductive effort (Figure 2e). The negative effects of massive seed production on carbohydrate reserves were thus mainly due to both the decrease in total leaf area and the increase in shoot respiration. The hydraulic conductivity and the PLC in the branchlets (8–10-mm diameter) and leaf mass per area were not affected by seed production (Figure 2i; Figure S6).

Approximately 1 month after the typhoon, its damage was estimated by the differences in traits before and after the typhoon (Figure 3). The total leaf area of shoots and the maximum photosynthetic rates in the remaining leaves exhibited significant decreases together with typhoon damage (evaluated by the increase in leaf electrolyte leakage) across the examined trees (Figure 3a,b). These decreases were due to intense wind and salt sprays, evidenced by the fact that the typhoon damage observed in the top canopies was obviously more severe on the windward sea side than on the leeward land side (Figure 1b). The starch stored within the sapwood decreased in most of the trees examined; however, the decrease in starch was not correlated with typhoon damage (Figure 3c) because individual trees with low starch reserves when the typhoon hit did not show further decreased starch concentrations. Typhoon damage decreased the hydraulic conductivity (K_{branch}) of branchlets (8–10-mm diameter; Figure 3d); however, this was not associated with an increase in the PLC, indicating that the decrease in K_{branch} was not related to air-induced embolism in xylem conduits (Figure S7b).

In the next spring, we examined the mortality rates of branchlets during the 5-month periods following the typhoon (Figure 4). The branchlets broken by intense winds were not included in the current mortality. The mortality rates gradually decreased with branch diameter (Figure 4b). The statistical results of GLM models (see Table S3; Section 2) showed that the factors causing mortality varied among diameter classes, depending on the reproductive effort and disasters. Reproductive effort was significantly correlated with the mortality of the distal branchlets (1–2-mm-diameter class; Figure 4a). The typhoon damage caused to leaves was significantly correlated with the mortalities of the branchlets of both the 1–2- and 3–4-mm-diameter classes (Figure 4a). The mortality of larger branchlets (8–10-mm-diameter class) was not correlated with either reproductive effort or typhoon damage but decreased significantly with the stored starch concentrations across the individual trees (Figure 4c). These data indicate that the mortality of larger branchlets was due to indirect effects of carbon starvation, rather than to direct effects caused by mass seed production and the typhoon.

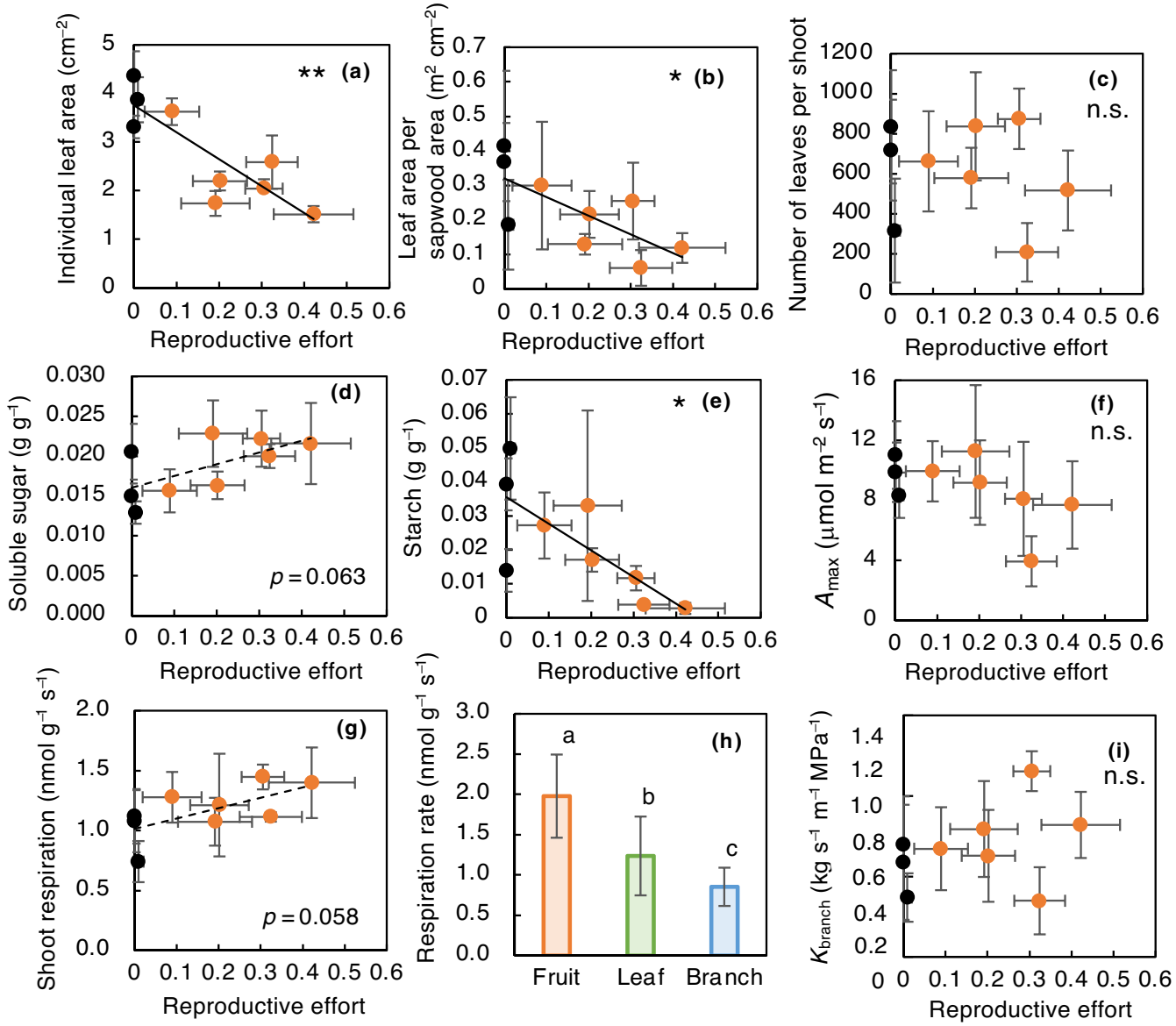

FIGURE 2 The seed production effects of nine individual trees examined before the typhoon hit. The reproductive effort on the x-axes indicates the ratio of fruit dry mass to total shoot dry mass (g g^{-1}). (a) The area of individual leaves. (b) The sapwood-area based total leaf area of shoots. (c) The number of leaves attached to shoots. (d) The concentrations of soluble sugars within the sapwood of the branchlets (8–10-mm diameter). (e) The concentrations of starch within the sapwood of the branchlets (8–10-mm diameter). (f) A_{max}: the leaf area-based maximum photosynthetic rates. (g) The dark respiration rates of shoots, including leaves, twigs, and fruits. The values are standardized to 26°C by using $Q_{10} = 2$. (h) Mass-based dark respiration rates of each tissue, including immature fruits, leaves, and twigs. Different letters show significant differences among the tissues. (i) K_{branch}: the sapwood area-based hydraulic conductivity in the branchlets (8–10-mm diameter). Mean and ±1 SD in each parameter for individual trees are shown. The solid lines show significant correlations ($p < 0.05$), and the dashed lines show marginal correlations ($0.05 \le p < 0.08$). $^{**}p < 0.01$, $^{*}p < 0.05$, n.s., non-significant ($p \ge 0.08$). Black circles show trees with no or almost no fruits

Approximately 8 months following the typhoon, a prolonged drought occurred in the early summer in 2020. The severe summer drought was evident from an extraordinary decrease in the predawn leaf water potential: the minimum value of −1.2 MPa in 2019 was recorded on August 3, while that of −3.3 MPa in 2020 was recorded on July 14 in the examined *D. lepidotum* trees (Figure S2). Persistent damage was still obviously observed in the top canopies at that time. Furthermore, large variations in new leaf emergence were found among the individual trees. The stored starch concentrations varied largely over time, as follows: the mean values (±1 SD) of the nine examined trees were 22.1 (±16.3) mg g^{-1} before the typhoon, 4.0 (±2.1) mg g^{-1} 1 month after the typhoon, and 11.2 (±8.8) mg g^{-1} at 8 months after the typhoon (Table S2). Thus, typhoon damage largely decreased the stored starch, and the starch concentrations did not entirely recover even in the next summer. During the 8-month period after the typhoon, the amounts of increases in the

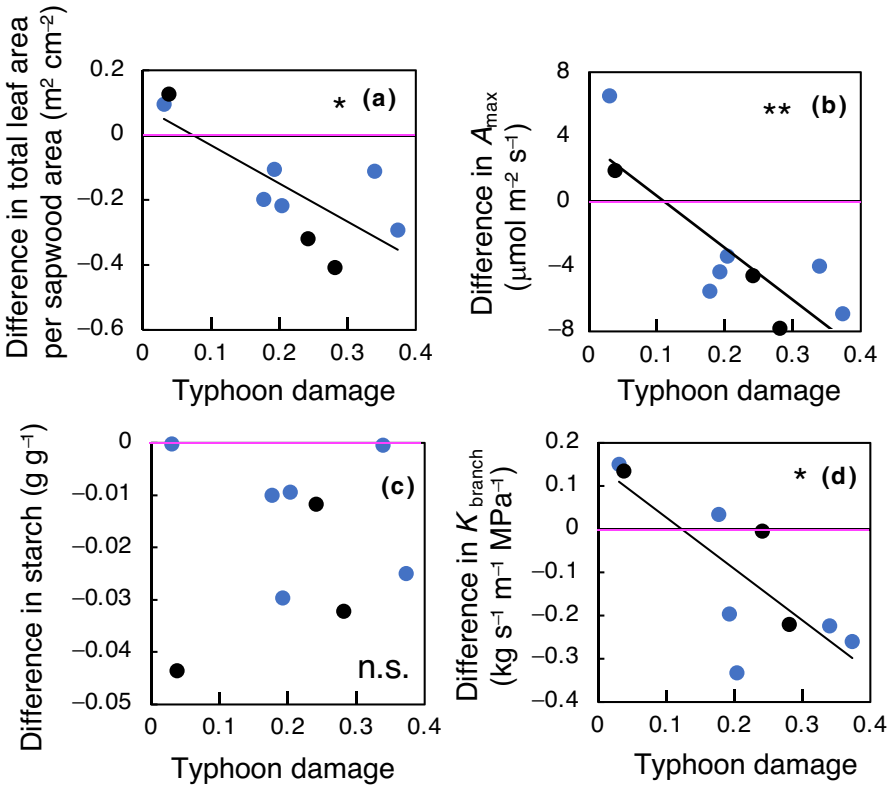

FIGURE 3 The typhoon damage of nine individual trees examined at approximately 1 month after the typhoon hit. The typhoon damage for each tree (*x*-axes) was measured by the differences in leaf electrolyte leakage before and after the typhoon. The *y*-axes indicate the differences in each trait before and after the typhoon. Negative values indicate the damage, not yet recovered, caused by the typhoon. (a) The total leaf area per sapwood area in shoots. (b) The leaf area-based maximum photosynthetic rates. (c) The concentrations of starch within the sapwood of the branchlets (8–10-mm diameter). (d) Sapwood area-based hydraulic conductivity in the branchlets. The solid lines show significant correlations ($p < 0.05$). $^{**}p < 0.01$, $^{*}p < 0.05$, n.s., non-significant ($p \geq 0.08$). Black circles show trees with no or almost no fruits

total area of leaves attached to shoots, the starch reserves, and the hydraulic conductivity in branchlets with 8–10-mm diameter (K_{branch}) were significantly ($p < 0.05$) or marginally ($p = 0.052$) correlated with the starch concentrations within branchlets 1 month following the typhoon across the examined trees (Figure 5). Because PLC marginally increased with decreasing stored starch ($p = 0.059$, Figure S6b), the decrease in K_{branch} during the severe summer drought could be related to air-induced xylem embolism. The long-term recoveries of leaf area, starch reserves, and hydraulics after typhoon damage were thus dependent on the starch reserves when the typhoon hit. The recovery of new leaf production was interrupted if the starch level was less than 1.8 mg g^{-1} (Figure 5a); the recovery of hydraulic conductivity was disrupted if the starch level was less than 5.4 mg g^{-1} (Figure 5c). These data show that there are starch concentration thresholds for the recovery of tree health. Therefore, drought resilience is dependent on carbohydrate reserves and is highly variable among individual trees. As a result, the recoveries of new leaf areas, starch reserves, and hydraulics after disasters are restricted by the previously stored starch levels. After the subsequent typhoon and drought events, even whole-plant death was found in several trees at the study site, especially in isolated *D. lepidotum* plants (Figure 6). Drought-induced tree death in *D. lepidotum* on islands is mainly due to carbon starvation (Saiki et al., 2017).

4 | DISCUSSION

Our findings are summarized in a schematic diagram describing the physiological processes of tree decline caused by the compound effects of typhoons and prolonged drought after masting (Figure 7). Representation of the physiological processes underlying tree decline by multiple climate extremes is a major priority for predicting the near-future compound hazards of forest ecosystems caused by long-term climate change and for developing global models. Massive seed production increased the mortality of distal canopy shoots (1–2-mm diameter) only and reduced the leaf size of individual leaves. Typhoon damage increased the mortality of larger canopy shoots (3–4-mm diameter) and decreased the total leaf area and photosynthetic capacity. These data show that climate extremes after masting resulted in decreases in the subsequent net carbon gain and stored starch within sapwood. If the levels of stored starch decreased below the corresponding thresholds, new leaf expansion and/or the recovery of branch hydraulics were completely interrupted. Consequently, their restoration of carbohydrate reserves was hindered, especially in trees with previously low starch reserves (see Figure 5b). We expect that tree death will occur if the stored starch becomes lower than these thresholds during recovery processes over the long term. Resprouting is important for tree survival after severe disturbance (Clarke et al., 2013; Pausas et al., 2015). However, resprouting requires a huge consumption of stored carbohydrates to compensate for their high carbon construction cost until trees have recovered their photosynthetic capacity (Chapin et al., 1990; Clarke et al., 2013). The cessation of new leaf expansion due to carbon starvation results in lingering damage; trees are not easily able to escape carbon starvation. If plant regrowth is disrupted, the physiological faculty of leaf photosynthesis and root water uptake decrease due to cell ageing, and living cells continuously reduce the stored carbohydrates by mitochondrial respiration in damaged trees (Saiki et al., 2017).

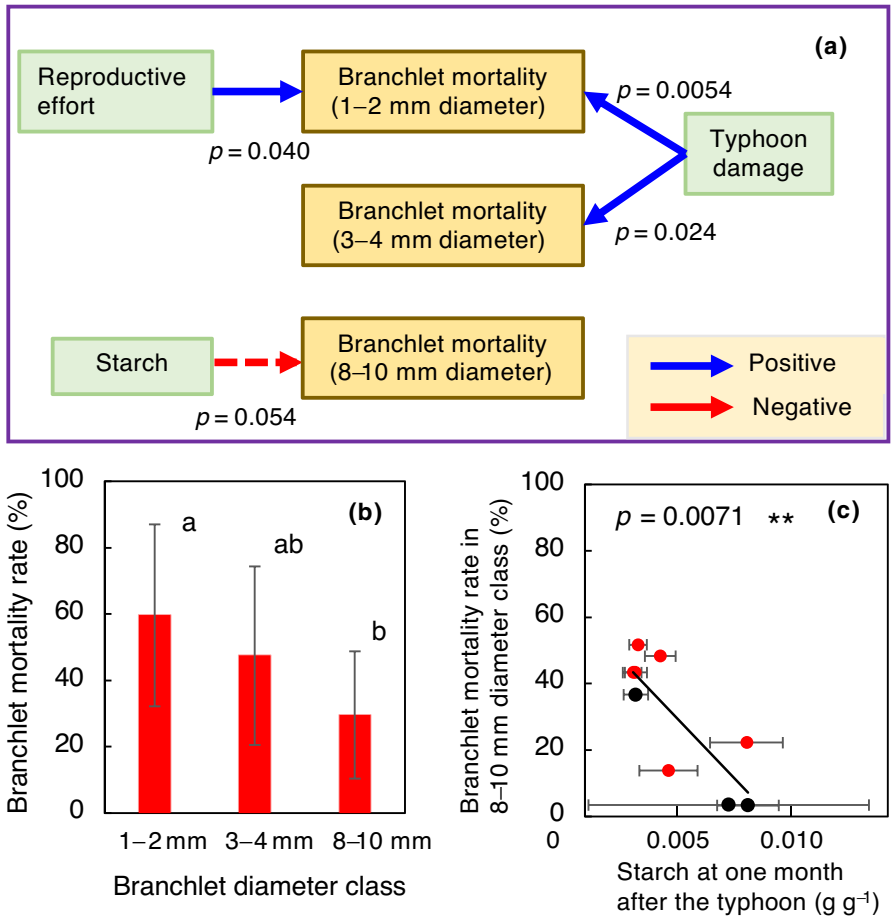

FIGURE 4 The mortality rates of branchlets during the approximately 5-month period after the typhoon hit. (a) The statistical results of the adequate general linear models with the lowest Akaike's information criterion values; the response variables were the mortality rates in each diameter class (1–2, 3–4, 8–10 mm) and the explanatory variables were the reproductive effort, the degrees of typhoon damage, and the starch concentrations in the 8–10-mm-diameter branchlets of the individual trees. (b) The mortality rates of branchlets in each diameter class. Different letters show significant differences among the classes. Mean and ±1 SD in each diameter class in all trees are shown. (c) The linear correlation between the mortality rates and the starch concentrations approximately 1 month after the typhoon within the sapwood of the branchlets of the 8–10-mm-diameter class ($p < 0.05$). Mean and ±1 SD in each parameter for individual trees are shown. Black circles show trees with no or almost no fruits

Stored carbohydrates are also used for physiological metabolism against various stresses and defense against pathogens and insects (Dunn et al., 1990; Old et al., 1990). With increasing drought conditions in the soil, the conversion from starch to soluble sugars progresses within sapwood in branchlets (Yoshimura et al., 2016), and soluble sugars are used to avoid dehydration through processes such as osmoregulation (Merchant et al., 2006) and the energy-driven refilling of embolized vessels under negative pressure in xylem conduits (Hacke et al., 2001; Liu et al., 2019; Nardini et al., 2011; Salleo et al., 2004; Secchi & Zwieniecki, 2011; Zwieniecki, & Holbrook, 2009). For the effective transport of carbohydrates from storage cells to metabolically active tissues during drought, the shrinkage of phloem cells caused by turgor collapse should be avoided (Dannoura et al., 2019; Hartmann, 2011; Sala et al., 2010; Salmon et al., 2019; Sevanto et al., 2014). Large defoliation decreases both water and carbon transport efficiencies, because of misshapen xylem vessels and the reduced diameter of phloem sieve tubes, respectively (Hillabrand et al., 2019). It has been shown that the level of starch within sapwood determines the "point of no return" for tree mortality in *Trema orientalis* (L.) Blume trees under drought on the islands (Kono et al., 2020). Carbohydrate reserves are thus crucial for mitigating stress and enhancing resilience. We hypothesize that delayed restoration of carbohydrate reserve levels fundamentally leads to synergistic impacts hindering the recovery of trees following compound damage by successive climate extremes after massive seed production.

The physiological mechanisms for masting signals are still controversial (Pearse et al., 2016). Based on a theoretical approach, a resource budget model regarding resource storage and reproductive costs has been proposed (Isagi et al., 1997). As the cue of mass flowering, some recent studies have indicated the role of storage of nitrogen rather than carbohydrates (Han et al., 2014; Miyazaki et al., 2014). The present study shows a negative correlation between reproductive efforts and stored starch (Figure 2e) but no significant

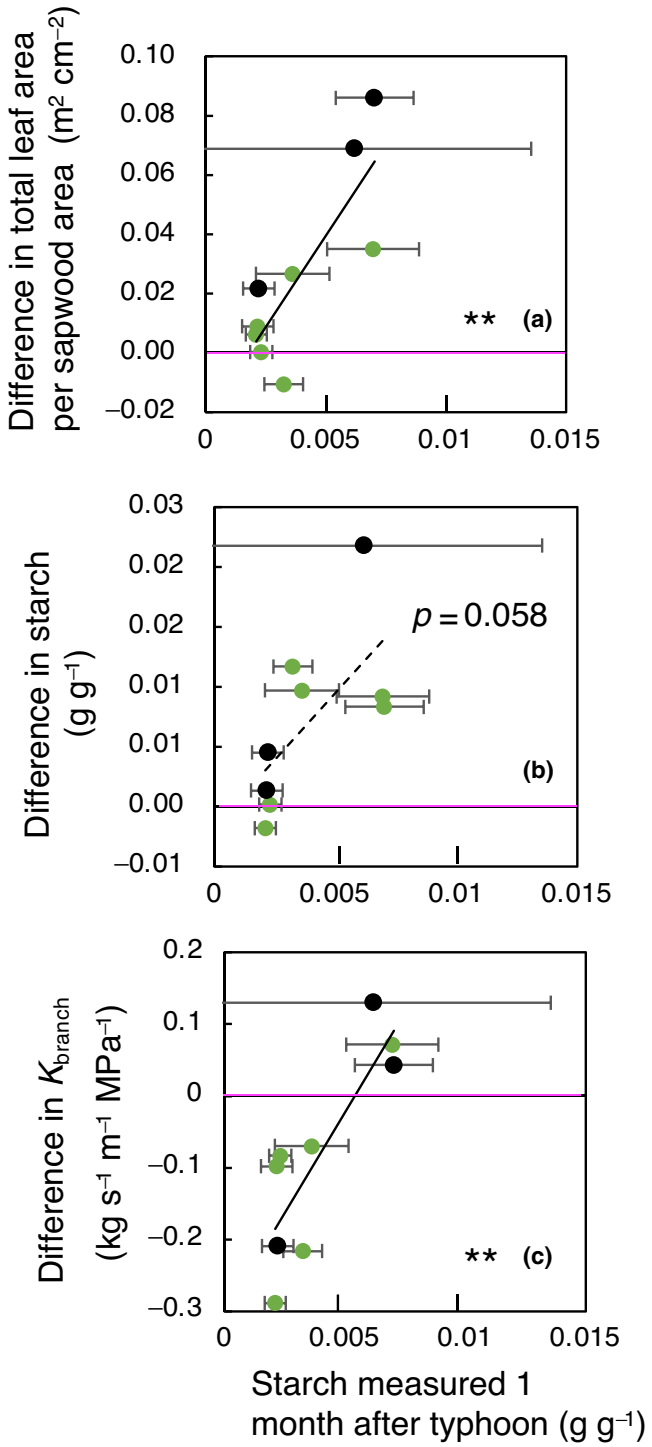

FIGURE 5 The recovery of leaf area, hydraulics, and starch reserves during the approximately 8 months after the typhoon. The *x*-axes are the starch concentrations within the sapwood of the branchlets (8–10 mm diameter) at approximately 1 month after the typhoon. The *y*-axes are the differences between approximately 1 and 8 months after the typhoon. Positive values show the recovery from typhoon damage, and negative values show a decline. (a) The sapwood-area based total leaf area. (b) The starch concentrations within the sapwood in the branchlets ($p = 0.052$). (c) The hydraulic conductivity in the branchlets (8–10 mm diameter). Mean and ±1 SD in each parameter for individual trees are shown. The solid lines show significant correlations ($p < 0.05$). $^{**}p < 0.01$. Black circles show trees with no or almost no fruits

correlation with photosynthetic rates (Figure 2f). However, canopy shoots with extreme seed production often have yellowish leaves with low photosynthetic rates (Figure S5; Figure 2f). Thus, even if masting is not directly connected with carbohydrate reserves, reduced photosynthetic capacity with depression of nitrogen within leaves can decrease the whole-plant carbohydrate reserves together with high seed respiration rates (Figure 2).

Our data indicate that the resilience of trees is ensured by the maintenance of high starch reserve levels. However, the faculty for storing carbohydrates within sapwood varies largely across tree species in relation to xylem anatomy because starch is mainly reserved within living parenchyma cells. The spatial trade-off among vessel, fiber, and parenchyma cells constrains various functions among tree species (Pratt & Jacobsen, 2017). Across angiosperm species, the increased parenchyma abundance is likely to lower the vessel and fiber abundance because of the trade-off constraint. With regard to hydraulics, across tree species, wood density is positively correlated with cavitation resistance against more negative pressure in xylem vessels (Hacke et al., 2001; Hoffmann et al., 2011). Therefore, there are functional trade-offs among hydraulic efficiency, cavitation resistance, storage function, and mechanical strength associated with different carbon and water use strategies across tree species (Ishida et al., 2008). Such trade-offs related to sapwood anatomy may suggest fundamental paradigms in physiological processes between carbon starvation and hydraulic failure to determine whether trees can survive under stressful environments (Kono et al., 2020). In the literature, the hydraulic failure hypothesis has been largely supported by evidence from mature trees (Davis et al., 2002; Rowland et al., 2015), whereas the carbon starvation hypothesis has been supported by evidence from tree seedlings (O'Brien et al., 2014) or small trees (Kono et al., 2020; Saiki et al., 2017; this study). However, why both hypotheses are supported in different cases remains unclear (Kono et al., 2020). In the present study, we used a small tree species, showing that the seed production significantly decreased carbohydrate reserves and that the level of stored starch strongly regulated tree growth and dieback. The significant negative correlation between seed production and starch in this study (Figure 2e) may be due to the small size of the trees with a low capacity for carbohydrate reserves, mostly leading to carbon starvation. Thus, tree size variations and ontogeny may also strongly affect the trade-offs between seed production and tree behavior, such as vegetative growth and stored carbohydrates.

Regrowth requires high carbon consumption for new shoot construction, especially after the trees undergo intensive defoliation. Therefore, the seasonal and yearly variations in carbohydrate reserve levels may be more dependent on the timing of growth and masting in individual trees than on functional types associated with the xylem anatomy and life-history strategy in angiosperm trees. This study also showed that the amount of stored starch varied largely among the individual trees before the typhoon hit (Figure 2; Table S2). The NSCs stored within sapwood in temperate woody plants vary widely seasonally and yearly (Furze et al., 2019; Richardson et al., 2012). These facts indicate that the mortality

FIGURE 6 Photos of dead trees in the survey area on the Ogasawara (Bonin) Islands. After the prolonged drought in summer in 2020, whole-plant death was found in several trees, especially in isolated plants of *Distylium lepidotum* Nakai. These photographs were taken on March 4 or 6, 2021

of trees following successive climate extremes will be dependent on the stochastic timing of the amount of carbohydrate reserves when disasters occur in forests. If masting largely reduces carbohydrate reserves and is entirely synchronized in almost all trees of a species, the subsequent climate extremes may intensively degrade the tree species in the forests. It has been demonstrated that repeated droughts cause more deleterious damage to gymnosperm trees than to angiosperm trees globally (Anderegg et al., 2020). The high resilience of angiosperm trees may be due to their high carbohydrate storage faculty, attributed to their rich content of parenchyma cells. Although angiosperm trees are usually globally predominant in temperate and tropical forests, we have little knowledge about the interspecific differences in vulnerability or resilience to global warming among angiosperm trees. Physiological comparisons among many angiosperm trees with respect to drought-induced forest dieback are still rare, especially in natural forests (Hoffmann et al., 2011; Rowland et al., 2015). Our data highlight that even in angiosperm trees, the compound hazard posed by successive climate extremes after masting is conspicuous, especially when tree carbohydrate reserves are lower than the threshold levels for resprouting and hydraulic recovery. Tree dieback in response to multiple events can diverge from that induced by a single event. Unfortunately, increased forest degradation may occur in the future because of the given projections of increases in the frequency and severity of tropical typhoons/cyclones and drought under ongoing global warming. Our results suggest that predictions regarding future changes in forest ecosystems are difficult because stored carbohydrate levels vary largely among individual trees over time and the synergistic impacts of climate extremes on tree health/resilience are dependent on the varying levels and the timing of carbohydrate reserves. The monitoring of carbohydrate reserves should thus be crucial for the

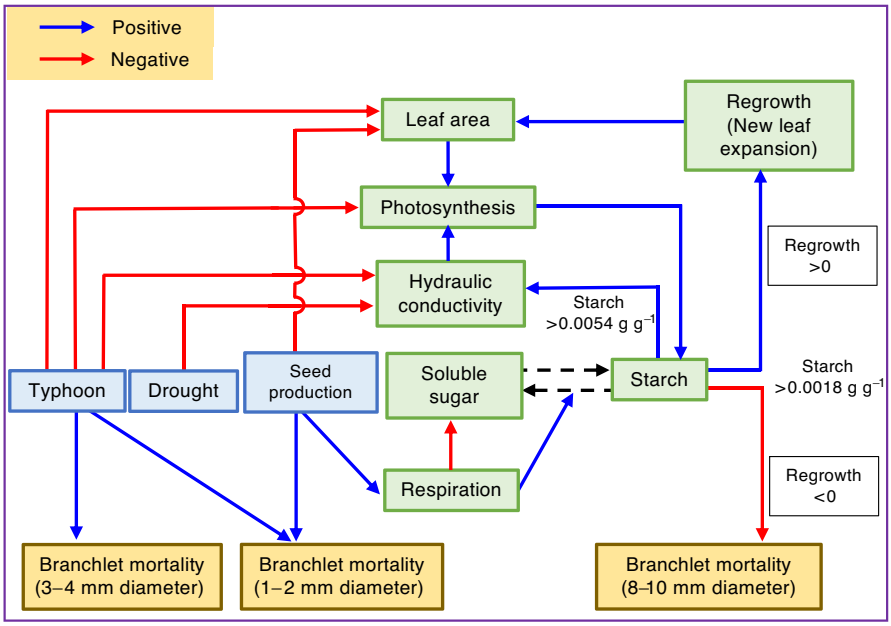

FIGURE 7 Schematic diagram of the physiological processes of tree decline caused by the compound effects of reproductive effort (seed production), the typhoon, and prolonged drought. The threshold of starch reserves for new leaf production was 1.8 mg g^{-1}, and for the recovery of hydraulic conductivity under prolonged drought, it was 5.4 mg g^{-1}. These threshold values were estimated in Figure 5a,c, respectively. Blue arrows show positive effects, and red arrows show negative effects. The dashed lines show the conversion between soluble sugar and starch. See the main text for more details

early detection of forest die-offs. Masting in predominant trees is often synchronized on a continental scale (Ascoli et al., 2017; Bogdziewicz et al., 2021; Vacchiano et al., 2017). With respect to masting and plant size, large trees have higher synchrony than small trees (Bogdziewicz, Szymkowiak, et al., 2020). If such masting largely decreases carbohydrate reserves even in large adult trees, climate extremes may lead to forest degradation in broad areas. Long-term monitoring of masting intervals and synchrony, carbohydrate reserves, and multiple climate extremes in various forests and biomes is thus important for detecting and predicting forest impacts under global climate change.

ACKNOWLEDGEMENTS

We thank Drs. N. Kachi, Y. Sano, M. Dannoura, T. Nakano, and K. Yoshimura for experimental support, Dr. T. Yasuda for drawing Figure S1, Mr. T. Suzuki for the field measurement of soil thickness, and Dr. D. Epron for his valuable comments. Permission for the field survey and plant collection was received form the Ministry of the Environment, the Forestry Agency, and the Ogasawara Islands Branch Office in the Tokyo Metropolitan Government, Bureau of General Affairs. This study was supported by grants-in-aid from the Japan Society for the Promotion of Science (nos. 16H02708 and 18H04149 to A.I.).

DATA AVAILABILITY STATEMENT

Data available on request from the authors.

ORCID

Atsushi Ishida https://orcid.org/0000-0003-0620-5819
Kiyosada Kawai https://orcid.org/0000-0001-8224-0515
Shin-Taro Saiki https://orcid.org/0000-0002-3685-2665
Kenichi Yazaki https://orcid.org/0000-0002-7649-4081
Jin Yoshimura https://orcid.org/0000-0003-1610-1386

REFERENCES

Abrams, M. D., & Nowacki, G. J. (2016). An interdisciplinary approach to better assess global change impacts and drought vulnerability on forest dynamics. *Tree Physiology*, *36*(4), 421–427. https://doi.org/10.1093/treephys/tpw005

Allen, C. D., Macalady, A. K., Chenchouni, H., Bachelet, D., McDowell, N., Vennetier, M., Kitzberger, T., Rigling, A., Breshears, D. D., Hogg, E. H. (T.)., Gonzalez, P., Fensham, R., Zhang, Z., Castro, J., Demidova, N., Lim, J.-H., Allard, G., Running, S. W., Semerci, A., & Cobb, N. (2010). A global overview of drought and heat-induced tree mortality reveals emerging climate change risks for forests. *Forrest Ecology and Management*, *259*(4), 660–684. https://doi.org/10.1016/j.foreco.2009.09.001

Anderegg, W. R. L., Berry, J. A., Smith, D. D., Sperry, J. S., Anderegg, L. D. L., & Field, C. B. (2012). The roles of hydraulic and carbon stress in a widespread climate-induced forest die-off. *Proceedings of the National Academy of Sciences of the United States of America*, *109*(1), 233–237. https://doi.org/10.1073/pnas.1107891109

Anderegg, W. R. L., Trugman, A. T., Badgley, G., Konings, A. G., & Shaw, J. (2020). Divergent forest sensitivity to repeated extreme droughts. *Nature Climate Change*, *10*(12), 1091–1095. https://doi.org/10.1038/s41558-020-00919-1

Ascoli, D., Vacchiano, G., Turco, M., Conedera, M., Drobyshev, I., Maringer, J., Motta, R., & Hacket-Pain, A. (2017). Inter-annual and decadal changes in teleconnections drive continental-scale synchronization of tree reproduction. *Nature Communications*, *8*, 2205. https://doi.org/10.1038/s41467-017-02348-9

Bell, G. (1980). The cost of reproduction and their consequences. *The American Naturalist*, *116*(1), 45–76. https://doi.org/10.1086/283611

Bennett, A. C., McDowell, N. G., Allen, C. D., & Anderson-Teixeira, K. J. (2015). Larger trees suffer most during drought in forests worldwide. *Nature Plants*, *1*(10), 15139. https://doi.org/10.1038/NPLANTS.2015.139

Blum, A., & Ebercon, A. (1981). Cell membrane stability as a measure of drought and heat tolerance in wheat. *Crop Science*, *21*(1), 43–47. https://doi.org/10.2135/cropsci1981.0011183X002100010013x

Bogdziewicz, M., Fernández-Martínez, M., Espelta, J. M., Ogaya, R., & Peñuelas, J. (2020). Is forest fecundity resistant to drought? Results from an 18-yr rainfall-reduction experiment. *New Phytologist*, *227*, 1073–1080. https://doi.org/10.1111/nph.16597

Bogdziewicz, M., Hacket-Pain, A., Ascoli, D., & Szymkowiak, J. (2021). Environmental variation drives continental-scale synchrony of European beech reproduction. *Ecology*, e03384. https://doi.org/10.1002/ecy.3384

Bogdziewicz, M., Szymkowiak, J., Calama, R., Crone, E. E., Espelta, J. M., Lesica, P., Marino, S., Steele, M. A., Tenhumberg, B., Tyre, A., Żywiec, M., & Kelly, D. (2020). Does masting scale with plant size? High reproductive variability and low synchrony in small and unproductive individuals. *Annals of Botany*, *126*(5), 971–979. https://doi.org/10.1093/aob/mcaa118

Chapin, F. S., Schulze, E.-D., & Mooney, H. A. (1990). The ecology and economics of storage in plants. *Annual Review of Ecology and Systematics*, *21*, 423–447. https://doi.org/10.1146/annurev.es.21.110190.002231

Clarke, P. J., Lawes, M. J., Midgley, J. J., Lamont, B. B., Ojeda, F., Burrows, G. E., Enright, N. J., & Knox, K. J. E. (2013). Resprouting as a key functional trait: how buds, protection and resource drive persistence after fire. *New Phytologist*, *197*(1), 19–35. https://doi.org/10.1111/nph.12001

Dannoura, M., Epron, D., Desalme, D., Massonnet, C., Tsuji, S., Plain, C., Priault, P., & Gérant, D. (2019). The impact of prolonged drought on phloem anatomy and phloem transport in young beech trees. *Tree Physiology*, *39*(2), 201–210. https://doi.org/10.1093/treephys/tpy070

Davis, S. D., Ewers, F. W., Sperry, J. S., Portwood, K. A., Crocker, M. C., & Adams, G. C. (2002). Shoot dieback during prolonged drought in *Ceanothus* (Rhamnaceae) chaparral of California: A possible case of hydraulic failure. *American Journal of Botany*, *89*(5), 820–828. https://doi.org/10.3732/ajb.89.5.820

Dubois, M., Gilles, K., Hamilton, J. K., Rebers, P. A., & Smith, F. (1951). A colorimetric method for the determination of sugars. *Nature*, *168*(4265), 167. https://doi.org/10.1038/168167a0

Dunn, J. P., Otter, D. A., & Kimmerer, T. W. (1990). Carbohydrate reserves, radial growth, and mechanisms of resistance of oak trees to phloem boring insects. *Oecologia*, *83*(4), 458–468. https://doi.org/10.1007/BF00317195

Fernández-Martínez, M., Belmonte, J., & Espelta, J. M. (2012). Masting in oaks: Disentangling the effect of flowering phenology, airborne pollen load and drought. *Acta Oecologia*, *43*, 51–59. https://doi.org/10.1016/j.actao.2012.05.006

Fernández-Martínez, M., & Peñuelas, J. (2011). Measuring temporal patterns in ecology: The case of mast seeding. *Ecology and Evolution*, *11*(7), 2990–2996. https://doi.org/10.1002/ece3.7291

Furze, M. E., Huggett, B. A., Aubrecht, D. M., Stolz, C. D., Carbone, M. S., & Richardson, A. D. (2019). Whole-tree nonstructural carbohydrate storage and seasonal dynamics in five temperate species. *New Phytologist*, *221*(3), 1466–1477. https://doi.org/10.1111/nph.15462

Hacke, U. G., Sperry, J. S., Pockman, W. T., Davis, S. D., & McCulloh, K. A. (2001). Trends in wood density and structure are linked to prevention of xylem implosion by negative pressure. *Oecologia*, *126*(4), 457–461. https://doi.org/10.1007/s004420100628

Han, Q., Kabeya, D., Iio, A., Inagaki, Y., & Kakubari, Y. (2014). Nitrogen storage dynamics are affected by masting events in *Fagus crenata*. *Oecologia*, *174*(3), 679–687. https://doi.org/10.1007/s00442-013-2824-3

Han, Q., Kabeya, D., Iio, A., & Kakubari, Y. (2011). Masting in *Fagus crenata* and its influence on nitrogen content and dry mass of winter buds. *Tree Physiology*, *28*(8), 1269–1276. https://doi.org/10.1093/treephys/28.8.1269

Hartmann, H. (2011). Will a 385 million year-struggle for light become a struggle for water and for carbon? How trees may cope with more frequent climate change-type drought events. *Global Change Biology*, *17*(1), 642–655. https://doi.org/10.1111/j.1365-2486.2010.02248.x

Hillabrand, R. M., Hacke, U. G., & Lieffers, V. J. (2019). Defoliation constrains xylem and phloem functionality. *Tree Physiology*, *39*(7), 1099–1108. https://doi.org/10.1093/treephys/tpz029

Hoffmann, W. A., Marchin, R. M., Abit, P., & Lau, O. L. (2011). Hydraulic failure and tree dieback are associated with high wood density in a temperate forest under extreme drought. *Global Change Biology*, *17*(8), 2731–2742. https://doi.org/10.1111/j.1365-2486.2011.02401.x

Isagi, Y., Sugimura, K., Sumida, A., & Ito, H. (1997). How does masting happen and synchronize? *Journal of Theoretical Biology*, *187*(21), 231–239. https://doi.org/10.1006/jtbi.1997.0442

Ishida, A., Nakano, T., Yazaki, K., Matsuki, S., Koike, N., Lauenstein, D. L., Shimizu, M., & Yamashita, N. (2008). Coordination between leaf and stem traits related to leaf carbon gain and hydraulics across 32 drought-tolerant angiosperms. *Oecologia*, *156*(1), 193–202. https://doi.org/10.1007/s00442-008-0965-6

Kabeya, D., Inagaki, Y., Noguchi, K., & Han, Q. (2017). Growth rate reduction causes a decline in the annual incremental trunk growth in masting *Fagus crenata* trees. *Tree Physiology*, *37*(10), 1444–1452. https://doi.org/10.1093/treephys/tpx081

Kelly, D., Geldenhuis, A., James, A., Holland, E. P., Plank, M. J., Brockie, R. E., Cowan, P. E., Harper, G. A., Lee, W. G., Maitland, M. J., Mark, A. F., Mills, J. A., Wilson, P. R., & Byrom, A. E. (2013). Of mast and mean: Differential-temperature cue makes mast seeding insensitive to climate change. *Ecology Letter*, *16*(1), 90–98. https://doi.org/10.1111/ele.12020

Kelly, D., & Sork, V. L. (2002). Mast seeding in perennial plants: Why, how, where? *Annual Review of Ecology and Systematics*, *33*(1), 427–447. https://doi.org/10.1146/annurev.ecolsys.33.020602.095433

Knops, J. M. H., Koeing, W. D., & Carmen, W. J. (2007). Negative correlation does not imply a tradeoff between growth and reproduction in California oaks. *Proceedings of the National Academy of Sciences of the United States of America*, *104*(43), 16982–16985. https://doi.org/10.1073/pnas.0704251104

Koenig, W. D., Knops, J. M. H., & Carmen, W. J. (2020). Can mast history be inferred from radial growth? A test using five species of California oaks. *Forest Ecology and Management*, *472*, 118233. https://doi.org/10.1016/j.foreco.2020.118233

Kono, Y., Ishida, A., Saiki, S.-T., Yoshimura, K., Dannoura, M., Yazaki, K., Kimura, F., Yoshimura, J., & Aikawa, S. (2020). Initial hydraulic failure followed by late-stage carbon starvation leads to drought-induced death in the tree *Trema orientalis*. *Communications Biology*, *2*, 8. https://doi.org/10.1038/s42003-018-0256-7

LaMontagne, J. M., Pearse, I. S., Greene, D. F., & Koenig, W. D. (2020). Mast seeding patterns are asynchronous at a continental scale. *Nature Plants*, *6*(5), 460–465. https://doi.org/10.1038/s41477-020-0647-x

Liu, J., Gu, L., Yu, Y., Huang, P., Wu, Z., Zhang, Q., Qian, Y., Wan, X., & Sun, Z. (2019). Corticular photosynthesis drives bark water uptake to refill embolized vessels in dehydrated branches of *Salix matsudana*. *Plant Cell and Environment*, *42*(9), 2584–2596. https://doi.org/10.1111/pce.13578

McDowell, N., Pockman, W. T., Allen, C. D., Breshears, D. D., Cobb, N., Kolb, T., Plaut, J., Sperry, J., West, A., Williams, D. G., & Yepez, E. A. (2008). Mechanisms of plant survival and mortality during drought: Why do some plants survive while others succumb to drought? *New Phytologist*, *178*(4), 719–739. https://doi.org/10.1111/j.1469-8137.2008.02436.x

McDowell, S. C. L., McDowell, N. G., Marshall, J. D., & Hultine, K. (2000). Carbon and nitrogen allocation to male and female reproduction in Rocky Mountain Douglas-fir (*Pseudotuga menziesii* var. *glauca*, Pinaceae). *American Journal of Botany*, *87*(4), 539–546. https://doi.org/10.2307/2656598

Merchant, A., Tausz, M., Arndt, S. K., & Adams, M. A. (2006). Cyclitols and carbohydrates in leaves and roots of 13 *Eucalyptus* species suggest contrasting physiological responses to water deficit. *Plant, Cell and Environment*, *29*(11), 2017–2029. https://doi.org/10.1111/j.1365-3040.2006.01577.x

Miyazaki, Y. (2013). Dynamics of internal carbon resources during masting behavior in trees. *Ecological Research*, *28*(2), 143–150. https://doi.org/10.1007/s11284-011-0892-6

Miyazaki, Y., Maruyama, Y., Chiba, Y., Kobayashi, M. J., Joseph, B., Shimizu, K. K., Mochida, K., Hiura, T., & Satake, A. (2014). Nitrogen is a key regulator of flowering in *Fagus crenata*: Understanding the physiological mechanism of masting by gene expression analysis. *Ecology Letter*, *17*(10), 1299–1309. https://doi.org/10.1111/ele.12338

Morita, Y. (1981). The dark-red forest soils of the Ogasawara Islands. (I) Site condition, and morphological, mechanical and chemical properties (in Japanese with English abstract). *Journal of the Japanese Forestry Society*, *63*(1), 1–7.

Nardini, A., Battistuzzo, M., & Savi, T. (2013). Shoot desiccation and hydraulic failure in temperate woody angiosperms during an extreme summer drought. *New Phytologist*, *200*(2), 322–329. https://doi.org/10.1111/nph.12288

Nardini, A., Lo Gullo, M. A., & Salleo, S. (2011). Refilling embolized xylem conduits: Is it a matter of phloem unloading? *Plant Science*, *180*(4), 604–611. https://doi.org/10.1016/j.plantsci.2010.12.011

Newell, E. A. (1991). Direct and delayed costs of reproduction in *Aesculus california*. *Journal of Ecology*, *79*(2), 365–378. https://doi.org/10.2307/2260719

Obeso, J. R. (2002). The costs of reproduction in plants. *New Phytologist*, *155*(3), 321–348. https://doi.org/10.1046/j.1469-8137.2002.00477.x

O'Brien, M. J., Leuzinger, S., Philipson, C. D., Tay, J. A., & Hector, A. (2014). Drought survival of tropical tree seedlings enhanced by non-structural carbohydrate levels. *Nature Climate Change*, *4*(8), 710–714. https://doi.org/10.1038/NCLIMATE2281

Old, K. K., Gibbs, R., Craig, I., Myers, B. J., & Yuan, Z. Q. (1990). Effect of drought and defoliation on the susceptibility of eucalypts to cankers caused by *Endothia gyrosa* and *Botryoshaeria ribis*. *Australian Journal of Botany*, *38*(6), 571–581. https://doi.org/10.1071/BT9900571.

Oouchi, K., Yoshimura, J., Yoshimura, H., Mizuta, R., Kusunoki, S., & Noda, A. (2006). Tropical cyclone climatology in a global-warming climate as simulated in a 20 km-mesh global atmospheric model: Frequency and wind intensity analysis. *Journal of the Meteorological Society of Japan*, *84*(2), 259–276. https://doi.org/10.2151/jmsj.84.259

Pausas, J. G., Pratt, R. B., Keeley, J. E., Jacobsen, A. L., Ramirez, A. R., Vilagrosa, A., Paula, S., Kaneakua-Pia, I. N., & Davis, S. D. (2015). Towards understanding resprouting at the global scale. *New Phytologist*, *209*(3), 945–954. https://doi.org/10.1111/nph.13644

Pearse, I. S., Koenig, W. D., & Kelly, D. (2016). Mechanisms of mast seeding: Resources, weather, cues, and selection. *New Phytologists*, *212*(3), 546–562. https://doi.org/10.1111/noh.14114

Pearse, I. S., LaMontagne, J. M., & Koenig, W. D. (2017). Inter-annual variation in seed production has increased over time (1990–2014). *Proceedings of the Royal Society B: Biological Sciences*, *284*, 20171666. https://doi.org/10.1098/rspb.2017.1666

Pesendorfer, M. B., Bogdziewicz, M., Szymkowiak, J., Borowski, Z., Kantorowicz, W., Espelta, J. M., & Fernández-Martínez, M. (2020). Investigating the relationship between climate, stand age, and temporal trends in masting behavior of European forest trees. *Global Change Biology*, *26*(3), 1654–1667. https://doi.org/10.1111/gcb.14945

Pratt, R. B., & Jacobsen, A. L. (2017). Conflicting demands on angiosperm xylem: Tradeoffs among storage, transport and biomechanics. *Plant, Cell and Environment*, *40*(6), 897–913. https://doi.org/10.1111/pce.12862

R Development Core Team (2019). *R: A language and environment for statistical computing*. R Foundation for Statistical Computing. http://www.R-project.org/

Reichstein, M., Bahn, M., Ciais, P., Frank, D., Mahecha, M. D., Seneviratne, S. I., Zscheischler, J., Beer, C., Buchmann, N., Frank, D. C., Papale, D., Rammig, A., Smith, P., Thonicke, K., van der Velde, M., Vicca, S., Walz, A., & Wattenbach, M. (2013). Climate extremes and the carbon cycle. *Nature*, *500*, 287–295. https://doi.org/10.1038/nature12350

Richardson, A. D., Carbone, M. S., Keenan, T. F., Czimczik, C. I., Hollinger, D. Y., Murakami, P., Schaberg, P. G., & Xu, X. (2012). Seasonal dynamics and age of stemwood nonstructural carbohydrates in temperate forest trees. *New Phytologist*, *197*(3), 850–861. https://doi.org/10.1111/nph.12042

Rowland, L., da Costa, A. C. L., Galbraith, D. R., Oliveira, R. S., Binks, O. J., Oliveira, A. A. R., Pullen, A. M., Doughty, C. E., Metcalfe, D. B., Vasconcelos, S. S., Ferreira, L. V., Malhi, Y., Geace, J., Mencuccini, M., & Meir, P. (2015). Death from drought in tropical forests is triggered by hydraulics not carbon starvation. *Nature*, *528*, 119–122. https://doi.org/10.1038/nature15539

Saiki, S.-T., Ishida, A., Yoshimura, K., & Yazaki, K. (2017). Physiological mechanisms of drought-induced tree die-off in relation to carbon, hydraulic and respiratory stress in a drought-tolerant woody plant. *Scientific Reports*, *7*, 2995. https://doi.org/10.1038/s41598-017-03162-5

Sala, A., Piper, F., & Hoch, G. (2010). Physiological mechanisms of drought-induced tree mortality are far from being resolved. *New Phytologist*, *186*(2), 274–281. https://doi.org/10.1111/j.1469-8137.2009.03167.x

Salleo, S., Lo Gullo, M. A., Trifilò, P., & Nardini, A. (2004). New evidence for a role of vessel-associated cells and phloem in the rapid xylem refilling of cavitated stems of *Laurus nobilis* L. *Plant, Cell and Environment*, *27*(8), 1065–1076. https://doi.org/10.1111/j.1365-3040.2004.01211.x

Salmon, Y., Dietrich, L., Sevanto, S., Hölltä, T., Dannoura, M., & Epron, D. (2019). Drought impacts on tree phloem: From cell-level responses to ecological significance. *Tree Physiology*, *39*(2), 173–191. https://doi.org/10.1093/treephys/tpy153

Schneider, C. A., Rasband, W. S., & Eliceiri, K. W. (2012). NIH image to ImageJ: 25 years of image analysis. *Nature Methods*, *9*(7), 671–675. https://doi.org/10.1038/nmeth.2089

Secchi, F., & Zwieniecki, M. A. (2011). Sensing embolism in xylem vessels: The role of sucrose as a trigger for refilling. *Plant, Cell and Environment*, *34*(3), 514–524. https://doi.org/10.1111/j.1365-3040.2010.02259.x

Sevanto, S., McDowell, N. G., Dickman, T., Pangle, R., & Pockman, W. T. (2014). How do tree die? A test of the hydraulic failure and carbon starvation hypotheses. *Functional Ecology*, *37*(1), 153–161. https://doi.org/10.1111/pce.12141

Shibata, M., Masaki, T., Yagihashi, T., Shimada, T., & Saitoh, T. (2020). Decadal changes in masting behaviour of oak trees with rising temperature. *Journal of Ecology*, *108*(3), 1088–1100. https://doi.org/10.1111/1365-2745.13337

Sperry, J. S., Donnelly, J. R., & Tyree, M. T. (1988). A method for measuring hydraulic conductivity and embolism in xylem. *Plant, Cell and Environment*, *11*(1), 35–40. https://doi.org/10.1111/j.1365-3040.1988.tb01774.x

Vacchiano, G., Hacket-Pain, A., Turco, M., Motta, R., Maringer, J., Conedera, M., Drobyshev, I., & Ascoli, D. (2017). Spatial patterns and broad-scale weather cues of beech mast seeding in Europe. *New Phytologist*, *215*(2), 595–608. https://doi.org/10.1111/nph.14600

Vergotti, M. J., Fernández-Martínez, M., Kefauver, S. C., Janssens, I. A., & Peñuelas, J. (2019). Weather and trade-offs between growth and reproduction regulate fruit production in European forests. *Agricultural and Forest Meteorology*, *279*, 107711. https://doi.org/10.1016/j.agrformet.2019.107711

Williams, A. P., Allen, C. D., Macalady, A. K., Griffin, D., Woodhouse, C. A., Meko, D. M., Swetnam, T. W., Rauscher, S. A., Seager, R., Grissino-Mayer, H. D., Dean, J. S., Cook, E. R., Gangodagamage, C., Cai, M., & McDowell, N. G. (2013). Temperature as a potential driver of

regional forest drought stress and tree mortality. *Nature Climate Change*, *3*(3), 292–297. https://doi.org/10.1038/nclimate1693

Xu, C., McDowell, N. G., Fisher, R. A., Wei, L., Sevanto, S., Christoffersen, B. O., Weng, E., & Middleton, R. S. (2019). Increasing impacts of extreme droughts on vegetation productivity under climate change. *Nature Climate Change*, *9*(12), 948–953. https://doi.org/10.1038/s41558-019-0630-6

Yoshimura, K., Saiki, S.-T., Yazaki, K., Ogasa, M. Y., Shirai, M., Nakano, T., Yoshimura, J., & Ishida, A. (2016). The dynamics of carbon stored in xylem sapwood to drought-induced hydraulic stress in mature tree. *Scientific Reports*, *6*, 24513. https://doi.org/10.1038/srep24513

Zeppel, M. J. B., Anderegg, W. R. L., & Adams, H. D. (2013). Forest mortality due to drought: Latest insights, evidence and unresolved questions on physiological pathways and consequences of tree death. *New Phytologist*, *197*(2), 372–374. https://doi.org/10.1111/nph.12090

Zwieniecki, M. A., & Holbrook, N. M. (2009). Confronting Maxwell's demon: Biophysics of xylem embolism repair. *Trends in Plant Sciences*, *14*(10), 530–534. https://doi.org/10.1016/j.tplants.2009.07.002

SUPPORTING INFORMATION

Additional supporting information may be found online in the Supporting Information section.

How to cite this article: Nakamura, T., Ishida, A., Kawai, K., Minagi, K., Saiki, S.-T., Yazaki, K., & Yoshimura, J. (2021). Tree hazards compounded by successive climate extremes after masting in a small endemic tree, *Distylium lepidotum*, on subtropical islands in Japan. *Global Change Biology*, 27, 5094–5108. https://doi.org/10.1111/gcb.15764

Tree hazards compounded by successive climate extremes after masting in a small endemic tree, *Distylium lepidotum*, on subtropical islands in Japan

TOMOMI NAKAMURA, ATSUSHI ISHIDA, KIYOSADA KAWAI, KANJI MINAGI, SHIN-TARO SAIKI, KENICHI YAZAKI, JIN YOSHIMURA

Table S1. Sizes of individual *Distylium lepidotum* Nakai trees, the thickness of their surrounding soils, reproductive effort, and the typhoon damage. The top-canopy heights above the ground surface, the stem diameters at 10% height of the top-canopy heights, the soil thickness near the stem bases, the masting level (mean ± 1 S.D.), and typhoon damage were observed for the individual trees examined.

Individual tree No.	The top-canopy height	Stem diameter	Soil thickness	Reproductive effort	Typhoon damage
	(m)	(cm)	(cm)	(g g-1)	
No. 1	2.51	6.21	25	0.202 ± 0.070	0.178
No. 2	2.37	5.97	25	0.422 ± 0.102	0.340
No. 3	2.17	5.17	85	0.191 ± 0.088	0.193
No. 4	2.35	5.63	102	0	0.242
No. 5	1.93	5.60	30	0	0.282
No. 6	1.52	6.18	7	0.089 ± 0.070	0.373
No. 7	2.09	4.53	14	0.324 ± 0.074	0.031
No. 8	2.40	5.34	14	0.009 ± 0.012	0.039
No. 9	1.16	5.24	11	0.305 ± 0.051	0.204

Table S2. The concentrations of soluble sugar, starch, and nonstructural carbohydrates (NSCs) within the sapwood of 8-10 mm diameter branchlets, the hydraulic conductivity (K_{branch}) of 8-10 mm diameter branchlets, the shoot dark respiration rates, and the ratio of total leaf area to sapwood area. (**a**) The mean values (1 SD) before the typhoon in 2019. (**b**) The mean values (1 SD) one month after the typhoon (typhoon effects) in 2019. (**c**) The mean values (1 SD) eight months after the typhoon under prolonged drought in summer in 2020.

(**a**) Stored carbohydrates before the typhoon hit in 2019.

Individual tree No.	Soluble Sugar	Starch	NSCs	*K*branch	Shoot respiration	Leaf area/ Sapwood area
	$g\ g^{-1}$	$g\ g^{-1}$	$g\ g^{-1}$	$kg\ s^{-1}\ m^{-1}\ MPa^{-1}$	$nmol\ g^{-1}\ s^{-1}$	$m^2\ cm^{-2}$
No. 1	0.0163 (0.0019)	0.0170 (0.0034)	0.0334 (0.0016)	0.6274 (0.2854)	1.2126 (0.4283)	0.2162 (0.0677)
No. 2	0.0216 (0.0057)	0.0028 (0.0016)	0.0243 (0.0064)	0.8194 (0.2054)	1.3986 (0.2945)	0.1190 (0.0430)
No. 3	0.0228 (0.0047)	0.0330 (0.0280)	0.0558 (0.0255)	0.7941 (0.2979)	1.0737 (0.1995)	0.1297 (0.0298)
No. 4	0.0206 (0.0039)	0.0139 (0.0063)	0.0345 (0.0081)	0.5873 (0.3573)	1.1185 (0.2274)	0.3677 (0.1131)
No. 5	0.0150 (0.0018)	0.0393 (0.0076)	0.0543 (0.0078)	0.7000 (0.2967)	1.0781 (0.2591)	0.4144 (0.2173)
No. 6	0.0157 (0.0030)	0.0271 (0.0097)	0.0428 (0.0103)	0.6717 (0.2576)	1.2778 (0.2112)	0.2995 (0.1847)
No. 7	0.0200 (0.0018)	0.0038 (0.0007)	0.0238 (0.0021)	0.3482 (0.2085)	1.1135 (0.0390)	0.0612 (0.0517)
No. 8	0.0129 (0.0016)	0.0498 (0.0151)	0.0627 (0.0146)	0.3685 (0.1505)	0.7410 (0.1715)	0.1862 (0.1300)
No. 9	0.0222 (0.0041)	0.0117 (0.0036)	0.0338 (0.0070)	1.1534 (0.1238)	1.4468 (0.1033)	0.2547 (0.1111)
Mean (1 S.D.)	0.0185 (0.0047)	0.0225 (0.0185)	0.0410 (0.0168)	0.6879 (0.3145)	1.1712 (0.2971)	0.2389 (0.1598)

(**b**) Stored carbohydrates approximately one month after the typhoon in 2019 (typhoon effects).

Individual tree No.	Soluble Sugar	Starch	NSCs	*K*branch	Shoot Respiration	Old-leaf area /Sapwood area	New-leaf area /Sapwood area	Total leaf area /Sapwood area
	$g\ g^{-1}$	$g\ g^{-1}$	$g\ g^{-1}$	$kg\ s^{-1}\ m^{-1}\ MPa^{-1}$	$nmol\ g^{-1}\ s^{-1}$	$m^2\ cm^{-2}$	$m^2\ cm^{-2}$	$m^2\ cm^{-2}$
No. 1	0.0146 (0.0009)	0.0070 (0.0019)	0.0216 (0.0020)	0.6622 (0.2071)	0.8423 (0.2020)	0.0173 (0.0177)	0.0000 (0.0000)	0.0173 (0.0177)
No. 2	0.0170 (0.0030)	0.0023 (0.0005)	0.0193 (0.0031)	0.5957 (0.2274)	0.5344 (0.1674)	0.0065 (0.0050)	0.0000 (0.0000)	0.0065 (0.0050)
No. 3	0.0194 (0.0019)	0.0032 (0.0008)	0.0226 (0.0013)	0.5972 (0.1699)	1.2504 (0.1727)	0.0244 (0.0164)	0.0031 (0.0027)	0.0274 (0.0154)
No. 4	0.0116 (0.0048)	0.0022 (0.0007)	0.0138 (0.0052)	0.5828 (0.1731)	1.2150 (0.4791)	0.0482 (0.0464)	0.0059 (0.0033)	0.0541 (0.0488)
No. 5	0.0123 (0.0017)	0.0070 (0.0016)	0.0194 (0.0032)	0.4789 (0.0739)	1.0962 (0.3602)	0.0048 (0.0033)	0.0049 (0.0034)	0.0097 (0.0048)
No. 6	0.0114 (0.0012)	0.0021 (0.0004)	0.0135 (0.0012)	0.4113 (0.2279)	1.2220 (0.4859)	0.0072 (0.0125)	0.0104 (0.0119)	0.0176 (0.0244)
No. 7	0.0186 (0.0026)	0.0036 (0.0015)	0.0222 (0.0035)	0.4977 (0.0221)	1.1674 (0.2592)	0.1557 (0.0702)	0.0050 (0.0045)	0.1607 (0.0742)
No. 8	0.0170 (0.0021)	0.0062 (0.0074)	0.0232 (0.0088)	0.5032 (0.1520)	1.2204 (0.2643)	0.3123 (0.0426)	0.0674 (0.0523)	0.3797 (0.0949)
No. 9	0.0157 (0.0096)	0.0022 (0.0007)	0.0178 (0.0099)	0.8211 (0.2226)	1.0316 (0.1249)	0.0379 (0.0163)	0.0023 (0.0027)	0.0402 (0.0185)
Mean (1 S.D.)	0.0153 (0.0044)	0.0040 (0.0030)	0.0193 (0.0056)	0.5722 (0.1878)	1.0644 (0.3420)	0.0683 (0.1026)	0.0110 (0.0254)	0.0792 (0.1233)

(Table S2 continued.)

(**c**) Stored carbohydrates approximately eight months after the typhoon under prolonged drought in summer in 2020.

Individual tree No.	Soluble Sugar	Starch	NSCs	*K*branch	Shoot respiration	Leaf arae/ Sapwood area
	$g\ g^{-1}$	$g\ g^{-1}$	$g\ g^{-1}$	$kg\ s^{-1}\ m^{-1}\ MPa^{-1}$	$nmol\ g^{-1}\ s^{-1}$	$m^2\ cm^{-2}$
No. 1	0.0232 (0.0049)	0.0162 (0.0074)	0.0394 (0.0055)	0.7336 (0.1704)	0.8347 (0.0755)	0.0522 (0.0079)
No. 2	0.0283 (0.0050)	0.0025 (0.0034)	0.0307 (0.0066)	0.5124 (0.1186)	0.4996 (0.1786)	0.0067 (0.0073)
No. 3	0.0329 (0.0079)	0.0149 (0.0067)	0.0478 (0.0104)	0.3814 (0.1492)	0.5781 (0.1133)	0.0138 (0.0081)
No. 4	0.0297 (0.0080)	0.0067 (0.0057)	0.0364 (0.0090)	0.3739 (0.1071)	0.8507 (0.1067)	0.0699 (0.0462)
No. 5	0.0238 (0.0039)	0.0153 (0.0140)	0.0392 (0.0173)	0.5218 (0.1183)	0.8980 (0.1006)	0.0908 (0.0802)
No. 6	0.0238 (0.0073)	0.0003 (0.0005)	0.0241 (0.0070)	0.1230 (0.1103)	1.2548 (0.2175)	0.0135 (0.0089)
No. 7	0.0292 (0.0053)	0.0133 (0.0070)	0.0425 (0.0028)	0.4282 (0.1077)	1.2923 (0.0687)	0.1823 (0.0423)
No. 8	0.0217 (0.0024)	0.0280 (0.0194)	0.0497 (0.0175)	0.6329 (0.1020)	1.2731 (0.1212)	0.3811 (0.0854)
No. 9	0.0255 (0.0040)	0.0035 (0.0040)	0.0291 (0.0049)	0.7234 (0.1919)	1.2143 (0.1592)	0.0469 (0.0284)
Mean (1 S.D.)	0.0264 (0.0063)	0.0114 (0.0122)	0.0378 (0.0125)	0.4940 (0.2247)	0.9691 (0.3259)	0.0982 (0.1228)

Table S3. The results of GLMs to explain branchlet mortality rates. For response variables, the mortality rates of the branchlets with different diameter classes of 1-2 mm, 3-4 mm, and 8-10 mm are shown as Mort_1, Mort_2, and Mort_3, respectively. The explanatory variables include reproductive effort (Seed), typhoon damage (Typhoon), and starch concentrations one month following the typhoon (Starch). The best GLMs with the lowest AIC (blue colour) were selected for the mortality rates in each diameter class, and the estimated coefficients, standard error, *T* values, and *P* values are shown (**: $P < 0.01$, *: $P < 0.05$, marginal: $0.05 \leq P < 0.08$, n.s.: $P \geq 0.08$). (a) All models and (b) the selected models for each diameter class.

(**a**) All models

Response variable	Unit	Model	AIC
Mort_1 (1-2 mm)	%	Mort_1=Seed+Typhoon	77.4
Mort_1 (1-2 mm)	%	Mort_1=Seed+Typhoon+Starch	78.0
Mort_1 (1-2 mm)	%	Mort_1=Typhoon+Starch	81.1
Mort_1 (1-2 mm)	%	Mort_1=Typhoon	82.2
Mort_1 (1-2 mm)	%	Mort_1=Starch	85.9
Mort_1 (1-2 mm)	%	Mort_1=Seed+Starch	87.0
Mort_1 (1-2 mm)	%	Mort_1=Seed	87.8
Mort_1 (1-2 mm)	%	Mort_1=Intercept	88.1
Mort_2 (3-4 mm)	%	Mort_2=Seed+Typhoon	81.5
Mort_2 (3-4 mm)	%	Mort_2=Seed+Typhoon+Starch	82.0
Mort_2 (3-4 mm)	%	Mort_2=Typhoon+Starch	82.8
Mort_2 (3-4 mm)	%	Mort_2=Typhoon	83.9
Mort_2 (3-4 mm)	%	Mort_2=Starch	85.4
Mort_2 (3-4 mm)	%	Mort_2=Seed+Starch	86.7
Mort_2 (3-4 mm)	%	Mort_2=Seed	87.7
Mort_2 (3-4 mm)	%	Mort_2=Intercept	87.7
Mort_3 (8-10 mm)	%	Mort_3=Seed+Typhoon+Starch	72.7
Mort_3 (8-10 mm)	%	Mort_3=Typhoon+Starch	72.9
Mort_3 (8-10 mm)	%	Mort_3=Starch	73.7
Mort_3 (8-10 mm)	%	Mort_3=Seed+Starch	74.9
Mort_3 (8-10 mm)	%	Mort_3=Seed+Typhoon	78.1
Mort_3 (8-10 mm)	%	Mort_3=Typhoon	79.9
Mort_3 (8-10 mm)	%	Mort_3=Seed	81.3
Mort_3 (8-10 mm)	%	Mort_3=Intercept	81.7

(Table S3 continued.)

(**b**) The selected GLMs for the branchlet mortality rates for each diameter class. Blue-coloured traits are effective factors for mortality. **: $P < 0.01$, *: $P < 0.05$, marginal: $0.05 \leq P < 0.08$, n.s.: $P \geq 0.08$.

Response variable	Unit	AIC	Explanatory variables	Estimated coefficients	Standard error	*T*-values	*P*-values
Mort_1 (1-2 mm)	%	77.4	Intercept	8.58	11.27	0.76	n.s.
			Seed	82.28	31.51	2.61	*
			Typhoon	176.65	41.69	4.24	**
Mort_2 (3-4 mm)	%	81.5	Intercept	1.38	14.13	0.10	n.s.
			Seed	77.80	39.50	1.97	n.s.
			Typhoon	156.58	52.26	3.00	*
Mort_3 (8-10 mm)	%	72.7	Intercept	32.71	15.64	2.09	n.s.
			Seed	30.47	26.34	1.16	n.s.
			Typhoon	59.44	34.49	1.72	n.s.
			Starch	-5224.31	2080.73	-2.51	**0.054 (marginal)**

Table S4. List of *r*- and *P*-values in each linear regression analysis.

Explanatory variables	Response variables	Figure No.	*r* value	*P* value
Reproductive effort	Individual leaf area	Fig. 2a	-0.854	**0.003**
Reproductive effort	Leaf area/sapwood area	Fig. 2b	-0.719	**0.029**
Reproductive effort	Number of leaves	Fig. 2c	-0.191	0.622
Reproductive effort	Souble sugar	Fig. 2d	0.640	**0.063**
Reproductive effort	Starch	Fig. 2e	-0.755	**0.019**
Reproductive effort	*A*max	Fig. 2f	-0.589	0.095
Reproductive effort	Shoot respiration rates	Fig. 2g	0.649	**0.058**
Reproductive effort	*K*branch	Fig. 2i	0.366	0.333
Typhoon damage	Difference in leaf area	Fig. 3a	-0.771	**0.015**
Typhoon damage	Difference in *A*max	Fig. 3b	-0.837	**0.005**
Typhoon damage	Difference in starch	Fig. 3d	0.097	0.803
Typhoon damage	Difference in *K*branch	Fig. 3e	-0.779	**0.013**
Starch	Branch mortality	Fig. 4c	-0.817	**0.007**
Starch	Difference in leaf area	Fig. 5a	0.821	**0.007**
Starch	Difference in starch	Fig. 5b	0.660	**0.053**
Starch	Difference in *K*branch	Fig. 5c	0.843	**0.004**
Shoot dry mass	Fruit dry mass	Fig. S3e	0.628	**<0.001**
Reproductive effort	Leaf mass per area	Fig. S6a	0.356	0.347
Reproductive effort	PLC	Fig. S6b	-0.189	0.626
Typhoon damage	Difference in PLC	Fig. S7a	0.227	0.556
Starch	Difference in PLC	Fig. S7b	-0.648	**0.059**

Table S5. The parameter list for each tree used for the generalized linear models (GLMs).

Individual tree No.	Reproductive effort	Typhoon damage	Starch	Mort_1 (1-2 mm)	Mort_1 (3-4 mm)	Mort_1 (8-10 mm)
	(g g-1)		(g g-1)	(%)	(%)	(%)
No. 1	0.202	0.178	0.0070	61.957	60.000	22.222
No. 2	0.422	0.340	0.0023	93.939	82.653	51.724
No. 3	0.191	0.193	0.0032	79.000	62.245	48.276
No. 4	0	0.242	0.0022	65.263	58.586	36.667
No. 5	0	0.282	0.0070	47.475	17.172	3.333
No. 6	0.089	0.373	0.0021	81.443	70.707	43.333
No. 7	0.324	0.031	0.0036	44.330	26.531	13.793
No. 8	0.009	0.039	0.0062	0.000	1.010	3.448
No. 9	0.305	0.204	0.0022	62.921	48.000	43.333

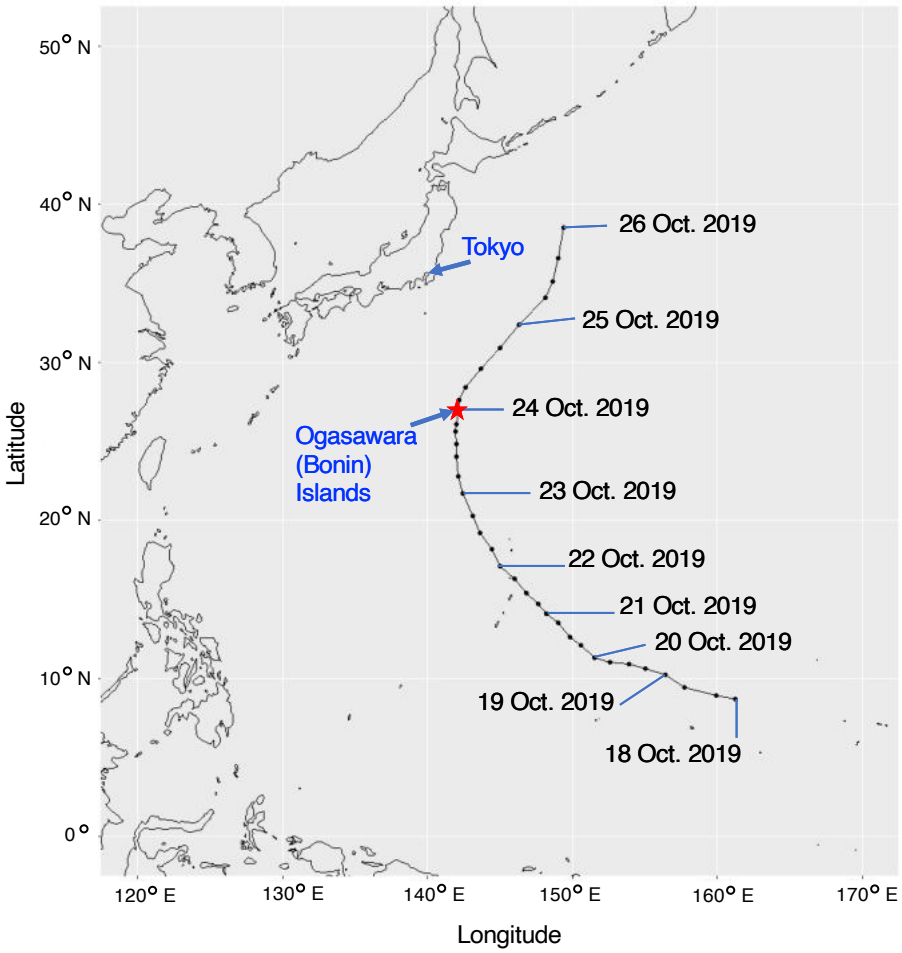

Fig. S1. The time course of typhoon "Bualoi". The typhoon hit the Ogasawara (Bonin) islands on 24 October 2019. The minimum air pressure was 963.5 hPa, and the instantaneous maximum wind speed on the islands was 52.7 m s^{-1}. This typhoon reached its peak intensity on 22 October, with 10-minute sustained winds of 51.4 m s^{-1}, 1-minute sustained winds of 72.2 m s^{-1}, and a central pressure of 935 hPa, consistent with a major Category 5 hurricane.

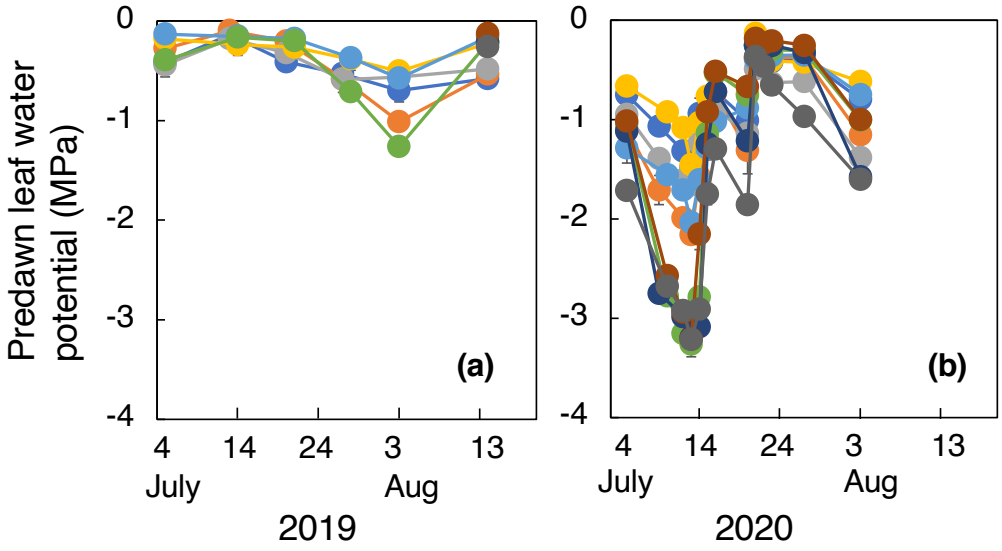

Fig. S2. The time course of predawn leaf water potential in the nine individual trees examined. The measurements were periodically conducted from early July to mid-August in the summers of 2019 (a) and 2020 (b).

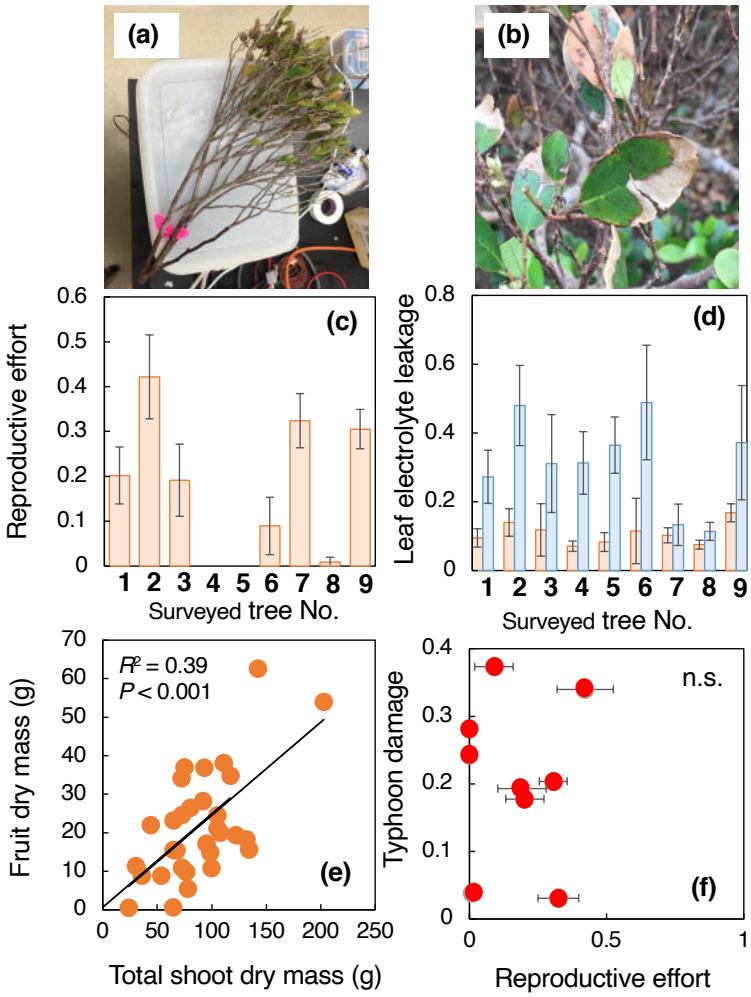

Fig. S3. Several measurements of shoots with various levels of masting and typhoon damage. (a) A photograph of a masting shoot with fruits (a cut shoot). (b) Photograph of leaves damaged by salt spray from sea water approximately one month after the typhoon. (c) The reproductive effort (fruit dry mass/total dry mass of shoots; g g^{-1}) for the individual trees. (d) The degree of typhoon damage (red bars: leaf electrolyte leakage before the typhoon; blue bars: leaf electrolyte leakage approximately one month after the typhoon). The differences in leaf electrolyte leakage before and after the typhoon were indicators of typhoon damage in the individual trees. (e) The correlations between the fruit dry mass and the total shoot dry mass in all cut shoots. The fruit mass-to-shoot mass ratio (i.e., slope) was used to represent the masting level of each shoot. (f) The relationship between reproductive effort and typhoon damage among the examined trees. There were no correlations between reproductive effort and typhoon damage. Black circles show trees with no or almost no fruits (No. 4, 5, and 8). (c), (d), (f) Mean and ± 1 S.D. in each parameter for individual trees are shown.

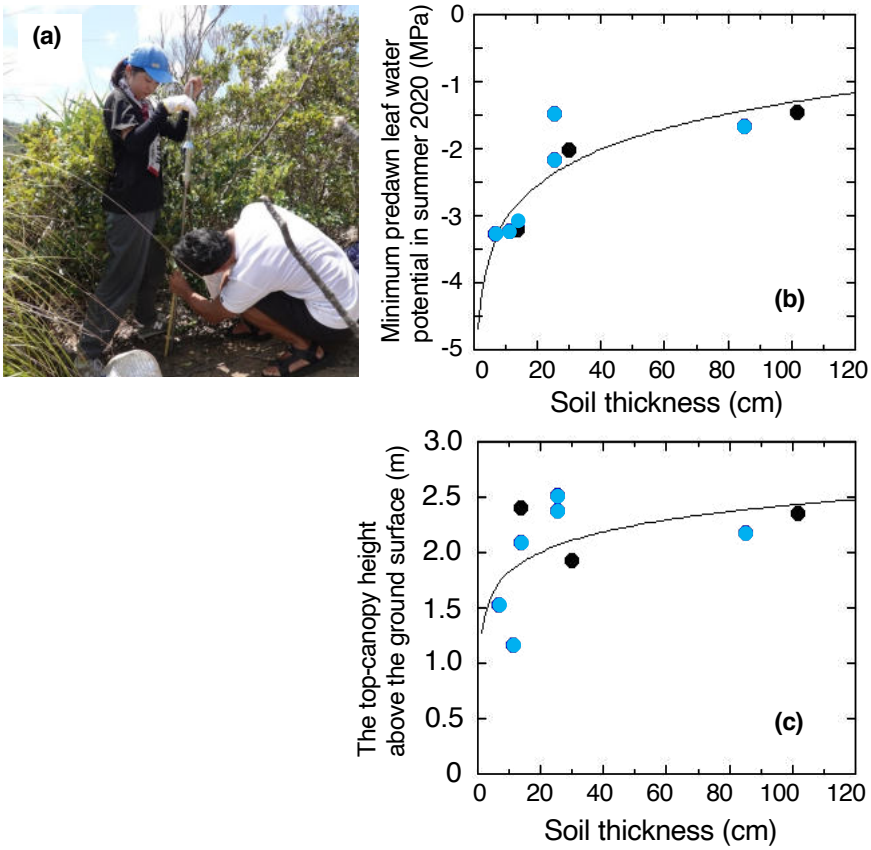

Fig. S4. The individual trees examined and their surrounding soil thickness. (a) A photograph of the field measurements of soil thickness. (b) The relationship between the soil thickness near the stem base and the minimum values of predawn leaf water potential in the dry summer of 2020. (c) The relationship between the soil thickness and the top-canopy heights above the ground surface among the examined trees. Blue circles show the fruiting trees, and black circles show trees with no or almost no fruits.

Fig. S5. The leaf colour of shoots with a high reproductive effort (fruit mass/shoot mass) changed to yellowish, showing low photosynthetic rates.

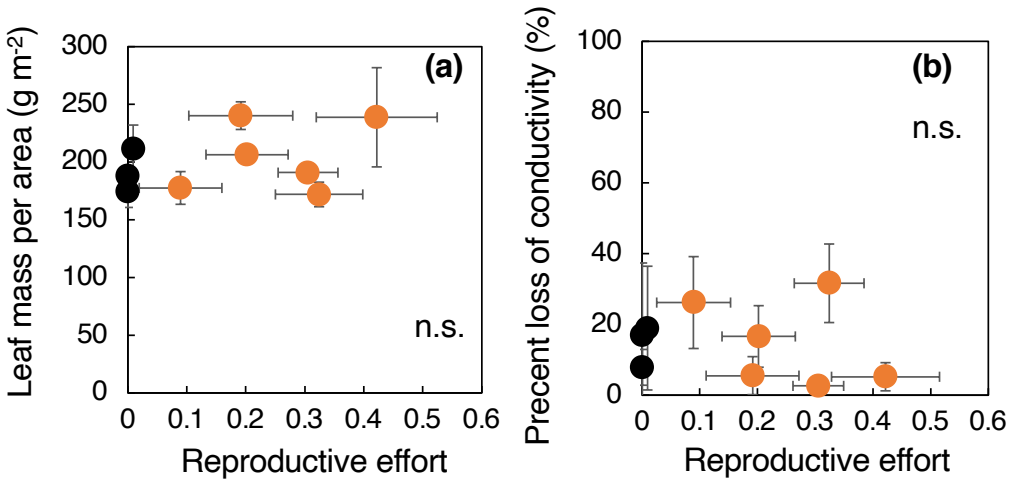

Fig. S6. The effects of reproductive effort were examined before the typhoon hits. The ratios of fruit dry mass to total shoot dry mass (x-axes) indicate the reproductive efforts of individual trees. (a) Leaf mass area (leaf dry mass/leaf area) of individual leaves. (b) The percent loss of conductivity in the branchlets (8-10 mm diameter). Black circles show trees with no or almost no fruits. Mean and ± 1 S.D. in each parameter for individual trees are shown.

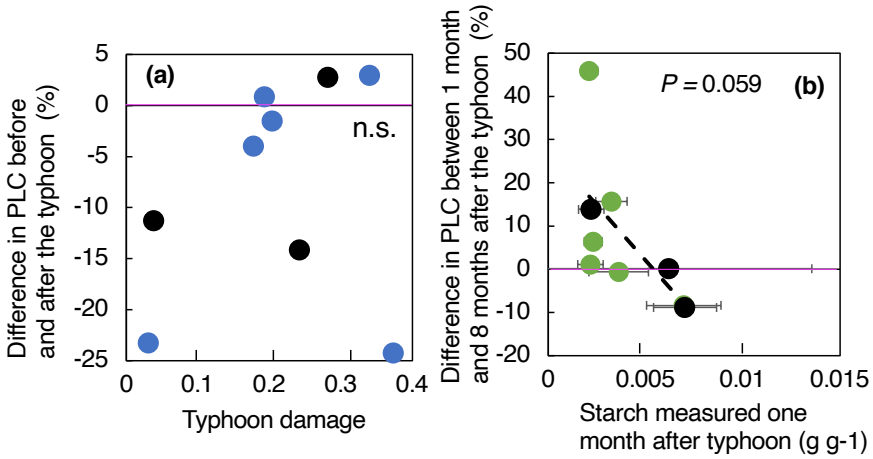

Fig. S7. The change in the percent loss of conductivity (PLC). (a) The differences in PLC before and one month after the typhoon. The x-axis indicates the degree of typhoon damage in the individual trees. (b) The differences in PLC between one month and eight months after the typhoon. The x-axis shows the starch concentrations approximately one month after the typhoon. Mean and ± 1 S.D. in each parameter for individual trees are shown. Black circles show trees with no or almost no fruits.